MYCOLOGIA

Mycologia

ISSN: (Print) (Online) Journal homepage: www.tandfonline.com/journals/umyc20

Morphological and phylogenetic resolution of *Conoideocrella luteorostrata* (Hypocreales: Clavicipitaceae), a potential biocontrol fungus for *Fiorinia externa* in United States Christmas tree production areas

Brian Lovett, Hana Barrett, Angie M. Macias, Jason E. Stajich, Lindsay R. Kasson & Matt T. Kasson

To cite this article: Brian Lovett, Hana Barrett, Angie M. Macias, Jason E. Stajich, Lindsay R. Kasson & Matt T. Kasson (2024) Morphological and phylogenetic resolution of *Conoideocrella luteorostrata* (Hypocreales: Clavicipitaceae), a potential biocontrol fungus for *Fiorinia externa* in United States Christmas tree production areas, Mycologia, 116:2, 267-290, DOI: 10.1080/00275514.2023.2296337

To link to this article: https://doi.org/10.1080/00275514.2023.2296337

MYCOLOGIA
2024, VOL. 116, NO. 2, 267–290
https://doi.org/10.1080/00275514.2023.2296337

Taylor & Francis
Taylor & Francis Group

Morphological and phylogenetic resolution of *Conoideocrella luteorostrata* (Hypocreales: Clavicipitaceae), a potential biocontrol fungus for *Fiorinia externa* in United States Christmas tree production areas

Brian Lovett[a], Hana Barrett[b], Angie M. Macias[c], Jason E. Stajich[d], Lindsay R. Kasson[e], and Matt T. Kasson[c]

[a]Emerging Pests and Pathogens Research Unit, Agricultural Research Service, United States Department of Agriculture, Ithaca, New York 14853; [b]Plant Pathology & Plant-Microbe Biology Section, School of Integrative Plant Science, Cornell University, Ithaca, New York 14853; [c]Division of Plant and Soil Sciences, West Virginia University, Morgantown, West Virginia 26506; [d]Department of Microbiology and Plant Pathology, University of California–Riverside, Riverside, California 92521; [e]School of Medicine, West Virginia University, Morgantown, West Virginia 26506

ABSTRACT

The entomopathogenic fungus *Conoideocrella luteorostrata* has recently been implicated in natural epizootics among exotic elongate hemlock scale (EHS) insects in Christmas tree farms in the eastern United States. Since 1913, *C. luteorostrata* has been reported from various plant feeding Hemiptera in the southeastern United States, but comprehensive morphological and phylogenetic studies of U.S. populations are lacking. The recovery of multiple strains of *C. luteorostrata* from mycosed EHS in North Carolina provided an opportunity to conduct pathogenicity assays and morphological and phylogenetic studies to investigate genus- and species-level boundaries among the Clavicipitaceae. Pathogenicity assays confirmed that *C. luteorostrata* causes mortality of EHS crawlers, an essential first step in developing this fungus as a biocontrol. Morphological studies revealed that conidia aligned with previous measurements of the *Paecilomyces*-like asexual state of *C. luteorostrata*, with conidiophore morphology consistent with historical observations. Additionally, a *Hirsutella*-like synanamorph was observed in select *C. luteorostrata* strains. In both a four-locus, 54-taxon Clavicipitaceae-wide phylogenetic analysis including D1–D2 domains of the nuclear 28S rRNA region (28S), elongation factor 1 alpha (*EF1-α*), DNA-directed RNA polymerase II subunit 1 (*RPB1*), and DNA-directed RNA polymerase II subunit 2 (*RPB2*) and a two-locus, 38-taxon (28S and *EF1-α*) phylogenetic analysis, all three *Conoideocrella* species were resolved as strongly supported monophyletic lineages across all loci and both methods (maximum likelihood and Bayesian inference) of phylogenetic inference except for 28S for *C. tenuis*. Despite the strong support for individual *Conoideocrella* species, none of the analyses supported the monophyly of *Conoideocrella* with the inclusion of *Dussiella*. Due to the paucity of *RPB1* and *RPB2* sequence data, *EF1-α* provided superior delimitation of intraspecies groupings for *Conoideocrella* and should be used in future studies. Further development of *C. luteorostrata* as a biocontrol against EHS will require additional surveys across diverse Hemiptera and expanded pathogenicity testing to clarify host range and efficacy of this fungus.

ARTICLE HISTORY
Received 11 October 2023
Accepted 14 December 2023

KEYWORDS
Paecilomyces cinnamomeus; Torrubiella luteorostrata; Dussiella tuberiformis; elongate hemlock scale; entomopathogenic fungus

INTRODUCTION

In the summer of 2020, the entomopathogenic fungus *Conoideocrella luteorostrata* [(Zimm.) D. Johnson, G.H. Sung, Hywel-Jones & Spatafora (Hypocreales: Clavicipitaceae)] (hereafter referred to as CL) was found causing an emergent epizootic on elongate hemlock scale insects (EHS; *Fiorinia externa*) infesting Fraser fir (*Abies fraseri*) trees on Christmas tree farms in North Carolina. EHS was first documented in the United States (U.S.) in 1908 on eastern hemlock (*Tsuga canadensis*) in New York State (Sasscer 1912), but this non-native pest has since spread throughout the eastern U.S. The range of EHS was originally limited by their cold sensitivity, but adaptations that increased cold tolerance emerged in the 1970s, which allowed for rapid northward expansion (Preisser et al. 2008).

Despite its name, confirmed plant hosts of EHS include spruce, fir, and pine species, in addition to eastern hemlock (McClure and Fergione 1977). Despite its long residency on native hemlock, EHS was first reported in Fraser fir tree farms in Yancey County, North Carolina, around 1993 (Miller and Davidson 2005; Sidebottom 2016). The damage inflicted by these insect pests on true fir tree farms and on eastern

CONTACT Matt T. Kasson mtkasson@mail.wvu.edu
Brian Lovett and Hana Barrett are co-first authors.
Supplemental data for this article can be accessed online at https://doi.org/10.1080/00275514.2023.2296337

Published online 26 Jan 2024

hemlock in native forested stands is challenging to quantify, but the spread of this insect, along with another non-native insect pest, hemlock woolly adelgid (HWA; *Adelges tsugae*), has been associated with defoliation and decline of hemlocks in the U.S. (Royle and Lathrop 2002). Given the broad host range of EHS, this pest poses significant risks to the Christmas tree production industry, where scale infection can decrease the ability of farmers to transport and sell their products across state lines (McClure and Fergione 1977), since the transport of Christmas trees can contribute to the spread of this and other non-native insect pests (Dale et al. 2020).

Chemical control has limited efficacy against EHS and other armored scales. Due to the high fertility of EHS and the vulnerability of their natural predators to chemical treatments, the pest population can rebound to higher levels after treatment (McClure 1977a). Fungal biocontrol agents have several characteristics that could be especially valuable for the management of EHS. Since entomopathogenic fungi produce diverse enzymes, toxins, and other secondary metabolites targeting their hosts as well as diverse mechanisms for overcoming host immune defenses, scales are unlikely to easily evolve resistance to fungal pathogens (Gao et al. 2017). Fungal biocontrol agents are often highly host specific, so they may have fewer nontarget effects than chemical pesticides (McClure 1977b). The fungus *Colletotrichum fioriniae* has been proposed as a biological control agent of EHS on eastern hemlock (Marcelino et al. 2009), but further research showed that it is primarily a leaf/stem endophyte (Martin and Peter 2021). *C. fioriniae* also has been reported as a postharvest pathogen of apples (Chechi et al. 2019), other fruits (Ivic et al. 2013; Ling et al. 2021), and native plants (Kasson et al. 2014), potentially limiting its potential as a biocontrol agent for EHS. Another putative fungal pathogen of elongate hemlock scale, *Metarhiziopsis microspora*, has also been described from the U.S. by Li et al. (2008), but its pathogenicity, ecology, and nontarget effects have not been further characterized. If a fungal biocontrol agent can be developed for EHS, it would be a valuable addition to an integrated pest management plan for Christmas tree growers. This biopesticide would also support resource managers of natural forested areas where eastern hemlock trees are succumbing to the cumulative effects of HWA and EHS.

In addition to confirmed epizootics in infested Fraser fir Christmas trees in North Carolina, CL also has been recently reported from mycosed EHS on these same hosts in Virginia and Michigan (Urbina and Ahmed 2022). Formerly known as *Torrubiella luteorostrata* (teleomorph or sexual form) or *Paecilomyces cinnamomeus* (PC; anamorph or asexual form), this fungus was first observed in the U.S. on whiteflies in Louisiana in 1913, followed by Mississippi in 1920, Alabama in 1923, and Florida in 1937 (TABLE 1; Samson 1974). Outside the U.S., both the asexual and sexual states of this fungus have been reported from several scale and whitefly species spanning three families in the hemipteran suborder Sternorrhyncha, from a total of 13 countries (including the U.S.) distributed across Africa (Ghana, Kenya, and Seychelles), Asia (China, Indonesia, Japan, Sri Lanka, and Thailand), North America (Cuba, Mexico, and the U.S.), Oceania (Samoa), and South America (Guatemala) (TABLE 1). Reports of CL in Russia are also known from numerous hosts, yet no morphological or DNA sequence data are available to resolve those populations among known *Conoideocrella* species. Herbarium specimens for CL also exist in public collections (SUPPLEMENTARY TABLE 1) for additional countries including Fiji, New Zealand, and Portugal, but no morphological data or DNA sequence data are available, nor were these specimens used in any taxonomic studies on the genus to confirm tentative identifications (TABLE 1). Nevertheless, these publicly archived herbarium specimens represent the only records for CL on members of the families Coccidae and Aleyrodidae in the U.S. and push back the first occurrence of this fungus in the U.S. by more than a century (TABLE 1). One of the commonly reported insect hosts for PC in the early 20th century, *Dialeurodes citri* or citrus whitefly, was itself introduced into Florida from Southeast Asia sometime between 1858 and 1885 (Morrill and Back 1911) and may have harbored CL upon arrival.

The genus *Conoideocrella* contains three formally described species: *C. tenuis* (Petch) (Johnson et al. 2009) (CT), *C. krungchingensis* (Mongkolsamrit et al. 2016) (CK), and *C. luteorostrata* (Schoch et al. 2020). CL is commonly found infecting multiple pest species in the hemipteran suborder Sternorrhyncha, including armored scale insects (Diaspididae), soft scales (Coccidae), and whiteflies (Aleyrodidae), whereas CK has only been reported from Diaspididae from Thailand. CT infects hosts from Aleyrodidae and Diaspididae, but across a limited geographic area, mostly confined to Southeast Asia (TABLE 1). CL forms characteristic ochre- to cinnamon-colored stromata upon infected insect hosts, with hypothalli consisting of thin hyphae expanding outward radially upon which conidiophores and/or perithecia are formed. CT and CK also produce variously colored stromata and hypothalli, but they also have features that are distinct

Table 1. Currently accepted *Conoideocrella* spp. and *Dussiella* spp., host information, and locality data based on molecular and morphological data and publicly available herbarium specimens.

					Previously reported strain localities[f]		
Species	Synonyms	Host order[b]	Host family	Host species	Molecular studies[c]	Morphological studies[d]	Herbarium specimens[e]
Conoideocrella luteorostrata (Zimm.) Johnson et al. 2009	*Torrubiella luteorostrata, Paecilomyces cinnamomeus, Verticillium cinnamomeum, Verticillium heterocladum, Torrubiella brunnea* (?)[a]	Hemiptera	Aleyrodidae (whiteflies)	Unresolved	Thailand	Seychelles; Sri Lanka (1889); USA: Alabama (1923), Louisiana (1913)	USA: Florida (1934)
		Hemiptera	Aleyrodidae (whiteflies)	*Aleurocanthus camelliae*	Japan	—	—
		Hemiptera	Aleyrodidae (whiteflies)	*Aleurocanthus spiniferus*	China (AF368806)	—	—
		Hemiptera	Aleyrodidae (whiteflies)	*Dialeurodes citri*	—	USA: Florida (1937), Louisiana (1915), Mississippi (1920).	USA: Florida (1939)
		Hemiptera	Aleyrodidae (whiteflies)	*Metaleurodicus cardini*	—	—	USA: Florida (1933)
		Hemiptera	Coccidae (soft scales)	Unresolved	Cuba (AY526468); Kenya (AY526467)	Ghana (1972); Indonesia; Samoa	—
		Hemiptera	Coccidae (soft scales)	*Protopulvinaria pyriformis*	—	—	USA: Florida (1932)
		Hemiptera	Diaspididae (armored scales)	Unresolved	—	—	New Zealand (1951)
		Hemiptera	Diaspididae (armored scales)	*Aspidiotus destructor*	—	Cuba (1922)	—
		Hemiptera	Diaspididae (armored scales)	*Comstockiella sabalis*	—	—	USA: Florida (1932)
		Hemiptera	Diaspididae (armored scales)	*Fiorinia externa*	USA: North Carolina, Virginia	US: North Carolina (2023)	—
		Hemiptera	Diaspididae (armored scales)	*Pseudoparlatoria parlatorioides*	—	—	USA: Florida (1935)
		Hemiptera	Unresolved	Unresolved	—	Guatemala (1941)	Guatemala (1942)
		Unresolved	Unresolved	Unresolved	—	Cuba; Mexico	Fiji (1977), Portugal (1931); USA: Florida (1944)
Conoideocrella tenuis (Petch) Johnson et al. 2009	*Torrubiella tenuis*	Hemiptera	Unresolved	Unresolved	Thailand	Sri Lanka (1914)	Belize (2007)
		Hemiptera	Aleyrodidae	*Aleyrodes* sp.	—	Sri Lanka (1914)	—
		Hemiptera	Diaspididae	*Aspidiotus destructor*	—	Sri Lanka (1899)	—
Conoideocrella krungchingensis Mongkolsamrit et al. 2016		Hemiptera	Diaspididae	Unresolved	Thailand	—	—

(*Continued*)

Table 1. (Continued).

Species	Synonyms	Host order[b]	Host family	Host species	Previously reported strain localities[f]		
					Molecular studies[c]	Morphological studies[d]	Herbarium specimens[e]
Dussiella tuberiformis (Berk. & Ravenel) Pat. ex Sacc. 1890	*Echinodothis tuberiformis, Hypocrea tuberiformis, Hypocrella tuberiformis*	Hemiptera	Unresolved	Unresolved	USA: North Carolina	—	—
		Unresolved	Unresolved	Unresolved	USA: Alabama, Arkansas (OR162438)	USA: Alabama (1890–1891), South Carolina (1888–1889)	USA: Alabama (1891), Florida (1932), Maine (1896), New Jersey, North Carolina (1878), South Carolina (1891)
Dussiella orchideacearum Rick 1906	*Echinodothis orchideacearum*	—	—	—	—	—	Brazil (pre-1928)
Dussiella violacea Höhn 1907		—	—	—	—	—	—

Note. — denotes no data available.
[a]The taxonomic placement of *T. brunnae* remains uncertain, as Hywel-Jones (1993) questioned its inclusion by Petch (1923).
[b]Unresolved at the order level denotes either an ambiguous insect host or plant host only was provided, with no comments on possible insect association.
[c]Denotes strains for which sequences were used as part of this study (see TABLES 2 and 3 for NCBI GenBank accession data) or are publicly available (accession provided in table) and meet a top-hit threshold of >98% sequence similarity against other strains of that same species.
[d]Denotes that strains were formally examined for (Atkinson 1891; Petch 1923; Samson 1974; Hywel-Jones 1993, or Mongkolsamrit et al. 2016).
[e]Localities based on collections searchable through Mycoportal using species names and synonyms as queries (see SUPPLEMENTARY TABLE 1 for records).
[f]Excludes localities mentioned in peer-reviewed literature for which no morphological or molecular identifications or deposited herbarium specimens were reported, including Russia (see Gavrilov-Zimin and Borisov 2020 for summary of Russian insect hosts and localities).

from all previously published accounts of CL, including a *Hirsutella*-like asexual stage in CK with 3–4 transversely septate conidia produced singly and no anamorph observed for CT (Johnson et al. 2009; Saito et al. 2012; Mongkolsamrit et al. 2016).

Dussiella tuberiformis (Berk. & Ravenel) Pat. ex Sacc. (previously known as *Echinodothis tuberiformis* and *Hypocrea tuberiformis*)—a closely allied member of the Clavicipitaceae (Kepler et al. 2012)—also infects scale insects on switchcane (*Arundinaria tecta*) and has been historically reported from the southeastern U.S., including Alabama, Mississippi, North Carolina, and South Carolina (TABLE 1; Atkinson 1891; White et al. 2002; Koroch et al. 2004). Contemporary observations of *D. tuberiformis* exist on the community science platform iNaturalist.org, and despite some variability in their macroscopic features, the isolates are markedly distinct from *Conoideocrella* based on the formation of stroma with crowded aggregations of individual perithecia (Atkinson, 1891; SUPPLEMENTARY TABLE 2). Kepler et al. (2012) resolved *Dussiella* as sister to *Conoideocrella*. However, the phylogenetic position of *Dussiella* among *Conoideocrella* species and other members of the Clavicipitaceae remains unclear, given its absence from the recent taxonomic description of CK (Mongkolsamrit et al. 2016). Two other species of *Dussiella, D. orchideacearum* Rick 1906 and *D. violacea* Höhn 1907, have been previously described, but neither has publicly available sequence data to resolve their relationships among *Conoideocrella* and *D. tuberiformis* (TABLE 1).

Given the taxonomic uncertainty between *Conoideocrella and Dussiella*, and the potential of developing a U.S. strain of CL as a biocontrol agent against EHS and potentially against non-native whiteflies, this study was undertaken to (i) provide a comprehensive summary of previous work on these fungi; (ii) morphologically and phylogenetically resolve the recently discovered U.S. populations of CL among previously characterized *Conoideocrella* and *Dussiella*; and (iii) conduct pathogenicity testing on EHS to further explore CL development as a potential biocontrol agent against this invasive insect. Although numerous surveys around the globe have confirmed the presence of CL, CT, and CK on various hemipteran hosts, robust multilocus phylogenetic analyses coupled with formal investigation of pathogenicity of CL on armored scale insects has not been previously pursued.

MATERIALS AND METHODS

Surveying for fungal pathogens of elongate hemlock scale.—Fungal surveys targeting entomopathogenic fungi on elongate hemlock scale (EHS) were conducted at three sites in Ashe County, North Carolina (Vannoy Farm [VF], Upper Mountain [UM], and Deal Family Farm [BAF]), and two sites in Grayson County, Virginia (Mount Rogers [MR] and Mount Rogers Orchard [MRO]), in late August and early September 2020. Although VF and BAF are on private lands with limited access, a third site, UM, serves as a research station for North Carolina State University's College of Agriculture and Life Sciences and is publicly accessible for research. Coordinates associated with each sampling location are provided in SUPPLEMENTARY TABLE 3. All three of the North Carolina sampling locations were reported as moderate to heavy EHS infestations, and none were actively managed with chemical controls. EHS infestations had not been reported from either site at Mount Rogers prior to this survey. Infected EHS were identifiable by the distinct orange mat of hyphae covering the cadavers and were abundant, with multiple infected cadavers on each infested needle (FIG. 1 A–B). EHS-free branches were collected from all sites, as were branches with uninfected insects from the four EHS-positive sites and branches with mycosed insects from the three North Carolina sites. Samples were individually bagged, such that insects found among branches were also preserved by site to allow for subsequent examination.

Fungal isolations.—Fungi were cultured from EHS by removing the infected/mycosed nymph cadavers from fir needles with a sterile scalpel or teasing needle and placing them on a potato dextrose agar (PDA; Difco, Detroit, Michigan) plate supplemented with 0.1 g/L streptomycin and 0.01 g/L tetracycline (+ST) to suppress bacterial growth. Cultures were prepared from representative samples from each location with infected EHS. Single colonies emerging from plated infected nymphs up to 2 weeks post plating were subcultured and retained in pure culture until colonies were of sufficient size to compare morphotypes. A single dominant morphotype (~85% of all colonies) with morphological characteristics consistent with the *Paecilomyces*-like asexual state of CL, including ochre- to cinnamon-colored mycelia with verticillate conidiophores and the production of a reddish pigment secreted into the agar by the fungus (Saito et al. 2012), was observed and retained for further morphological and molecular investigation (FIG. 1).

Culture-based survey of fir needles.—Because other hemipteran entomopathogens, such as *Colletotrichum fioriniae* (EHS) and *Dussiella tuberiformis*, are known

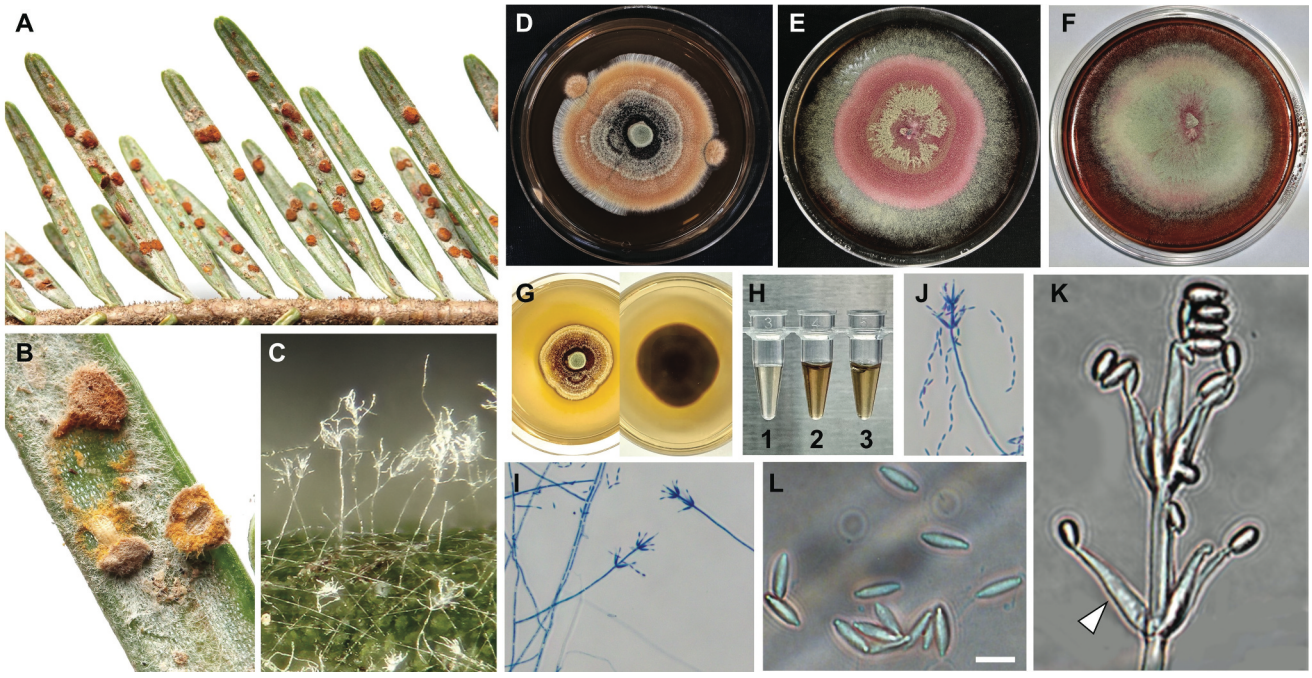

Figure 1. Natural infections (A–C), pure cultures (D–G), and select morphological features (I–L) including extracted pigments (H) from *C. luteorostrata* strains recovered from an epizootic on EHS infesting Fraser fir Christmas trees in North Carolina. Macroscopic features include orange stroma produced over killed elongate hemlock scale crawler cadavers on the underside of fir needles (A–B) and verticilliate condiophores (C) emerging from the white mycelium immediately surrounding the mycosed EHS. Representative cultures on PDA+ST at 1–2 weeks (D), 3–4 weeks (E), and 5 weeks (F) of age. Pigment production by CL on PDA (G) and following extraction from 1.78-cm-diameter colonized agar plugs from a >5-week-old culture with water (H1), ethanol (H2), and methanol (H3). Microscopic features include representative conidiophores (C, I–K) with phialides (white arrow, K), and conidia (J–L) mounted in lactic acid with and without cotton blue. (L) Bar = 5 µm. Photos in A–C are from Watauga County, North Carolina, and taken by Dr. Matt Bertone. Reproduced with permission.

leaf endophytes exhibiting epibiont growth on their plant hosts (White et al. 2002; Koroch et al. 2004; Martin and Peter 2021), we sought to determine whether CL could be reisolated from healthy and dead Fraser fir needles sampled from trees with and without EHS and/or CL. The culturable fungal communities of the fir needles were studied from trees and needles with no EHS, EHS only, and EHS infected with CL. A total of 60 needles were sampled across five previously referenced sampling sites. This included 24 live needle samples from six EHS+CL+ trees (UM and VF), 12 samples from three EHS+CL− trees (MRO), 12 samples from three EHS−CL− trees (BAF), and 12 dead needle samples from one EHS−CL − tree (MR) and two trees at BAF.

Needles were sterilized in 10% sodium hypochlorite for 20s followed by a sterile water rinse for 20s, placed on sterile filter paper to dry for 1 min, and then plated onto PDA+ST. Isolated fungi were retained in pure culture to compare morphotypes, and representatives of the most prevalent morphotypes along with any morphotypes that had morphological characteristics similar to CL were retained for sequencing.

Superficial survey for fungal infections in co-occurring arthropods.—To assess for potential nontarget (non-EHS) impacts, living and deceased nonsessile arthropods (i.e., insects, arachnids, and collembolans) found in EHS-infested and EHS-free Fraser fir branch materials were collected, examined under a dissecting scope for conspicuous fungal infections, and once determined to not have obvious outward fungal growth stored in ethanol for subsequent morphological identification. No fungal isolations were attempted from outwardly asymptomatic living arthropods collected during this survey, nor were collected dead arthropods, which lacked outward infections, incubated for fungal cultivation because CL produces conspicuous, dense growth on infected cadavers. A higher-level identification (i.e., class, subclass, or order) was assigned to all arthropods, and, where possible, a lower-level (down to species) identification was provided, leveraging resources such as BugGuide and iNaturalist (SUPPLEMENTARY TABLE 4).

Morphological studies.—A total of 13 CL strains recovered from mycosed EHS, spanning three locations in North Carolina, were assessed. Morphological studies

included sporulation observations, conidial measurements, and colony growth rates. One representative strain, CLUM14, was deposited in the Agricultural Research Service (ARS) Collection of Entomopathogenic Fungal Cultures (ARSEF) and will be referred to hereafter as ARSEF 14590.

Slides for measuring conidia were prepared from 2-week-old PDA+ST cultures of four CL strains: ARSEF 14590, UM11, VF11, and VF14. Slides were prepared with lactic acid as a mountant, sealed with clear nail polish, and stored flat for several weeks before measurements were conducted. Slides were examined and photographed using a Nikon Eclipse E600 compound microscope (Nikon Instruments, Melville, New York) equipped with a Nikon Digital Sight DS-Ri1 high-resolution microscope camera. Lengths and widths for 25 conidia for each strain were measured using Nikon NIS-Elements BR3.2 imaging software. Raw spore measurements are available in SUPPLEMENTARY TABLE 5.

Spore measurement data were analyzed using the packages TIDYVERSE (1.3.2; Wickham et al. 2019), AGRICOLAE (1.3.5; de Mendiburu 2021), RCOLORBREWER (1.1.3; Neuwirth 2022), SCALES (1.2.1; Wickham and Seidel 2022), CAR (3.1.2; Fox and Weisberg 2019), and VIRIDIS (0.6.2; Garnier et al. 2021) in R (4.2.2; R Core Team 2022). Normality was assessed using the Shapiro-Wilk test, and equality of variance was assessed using Levene's test. Analysis of variance (ANOVA) was performed to check for differences in spore measurements across strains, and Tukey's honest significance test was used to identify any significant pairwise differences. A P-value <0.05 was considered significant for all analyses. All data and code for analyses included in this paper are available on GitHub: https://github.com/HanaBarrett/EHS-CL-Analysis.

Colony growth rate was measured to determine temperature optima for CL strains from North Carolina. A sterile 1.78-cm-diameter cork borer was used to cut colonized agar plugs from 2-week-old fungal cultures of two strains: BAF14 and VF45. These agar plugs were plated in the center of 9-cm-diameter Petri plates containing PDA+ST. Five plates each for each of the two strains were placed in incubation chambers set to 10, 22, or 30 C and kept in complete darkness. The perimeter of the colony from the center of the Petri plate was marked along four predrawn radii (90, 180, 270, and 360 degrees) every 2 days. After 2 weeks, the distance between each point and the perimeter of the inoculation plug was measured and recorded. Average daily growth rate was calculated as half the distance of mean 2-day growth rate, the latter of which was the average of individual measurements from four radii (i.e., during days 4, 6, 8, 10, 12, and 14). Plates with satellite colonies or atypical radial growth were excluded. For isolates that showed no radial growth between successive time points at a given tested temperature, plates were still monitored for 14 days, after which plates were returned to 22 C to assess whether growth resumed. Raw colony growth measurements are available in SUPPLEMENTARY TABLE 6.

Alternative culturing methods to stimulate development of other additional spore types/asexual states (e.g., *Hirsutella*-like septate conidia reported in CK) and specialized fungal structures (e.g., appressoria) were initiated by observing growth upon a coverslip. This was initiated by two methods. ARSEF 14590 conidia were mixed into a cooling solution of PDA, after which a small volume (~5 µm) was placed on a sterile slide beneath a sterile coverslip. In another approach, a cube of stab-inoculated water agar was transferred similarly between a sterile slide and sterile coverslip (Rivalier and Seydel 1932; Villamizar et al. 2021). These were incubated for at least 2 weeks before they were observed directly, then coverslips were removed for staining and further observation. Furthermore, the fungus was grown in liquid culture in potato dextrose broth shaken at 150 rpm for 7 days in an attempt to trigger blastospore production.

Pathogenicity assays.—Branches with EHS crawlers with no outward evidence of fungal growth were collected from hemlock trees in Morgantown, West Virginia. As of December 2023, CL has not been confirmed anywhere in the state. Infested branchlets were randomized and distributed evenly into three replicates of two treatments: dipped completely into at least 20 mL of 10^7 CL conidia in water or dipped into sterile water as a control. To minimize strain-level variability, a composite inoculum consisting of three CL strains (ARSEF 14590, VF14, and BAF11) from the three CL-confirmed locations in North Carolina was used for all pathogenicity tests. Treated branchlets (2.5–3.5 cm in length) were fully submerged in inoculum or water for 10s. Branchlets were held at 22 C in Petri dishes in separate plastic containers for each treatment. Damp paper towels were provided in containers to maintain high relative humidity for insects and plants. These treatments were monitored daily for 13 days, except on day 9, to assess emergence and mortality. The results of this bioassay were subjected to Kaplan-Meier log-

rank survival analysis to test for significant differences in R (4.2.2) using the SURVIVAL package (Therneau 2022).

To demonstrate that CL isolated from EHS could reinfect healthy EHS, and thus fulfill Koch's postulates, the following methods were used. EHS-infested branches were stored at 22 C in a sealed container with a damp paper towel to encourage crawler development. Once sufficient crawlers had emerged after 2–4 days, crawlers were collected for infection assays. Fresh branchlets without EHS were prepared by dipping entirely into a 20-mL solution of 10^7 CL conidia (composite inoculum as described above) suspended in water, and branchlets were set into four Petri dishes. Then, 15 emerged crawlers for each of the four dishes were gently moved to each dish using a small, sterile paintbrush. Cadavers from the bioassay were removed 14 days later, surface-sterilized with 10% sodium hypochlorite for 10s, and plated on PDA+ST. The resulting isolates were identified through spore and colony morphology and sequencing of the internal transcribed spacer (ITS) region.

DNA extraction, PCR, and sequencing.—DNA was extracted from seven representative strains isolated from infected EHS crawlers across three sampling locations in Ashe County, North Carolina, using the protocol previously described by Macias et al. (2020). This included CL strains ARSEF 14590, BAF11, BAF14, UM11, VF11, VF41, and VF42. For genome sequencing of ARSEF 14590, DNA was extracted using a DNeasy PowerSoil Pro Kit (Qiagen, Maryland, USA) using manufacturer's protocols. Extracted DNA was stored at −20 C.

To confirm species identities for our strains and build a phylogeny for *Conoideocrella* and close allies, we first targeted sequencing of the universal fungal barcoding gene (the ribosomal internal transcribed spacer region of the rDNA (ITS), which includes ITS1, 5.8S, and ITS2), and the D1–D2 domains of the 28S rRNA gene (28S), for each of seven CL strains. Primer names, sequences, and polymerase chain reaction (PCR) programs are listed in SUPPLEMENTARY TABLE 7. PCR reagents and post-PCR cleanup are as described in Macias et al. (2020). The amplified purified products were Sanger-sequenced by Eurofins Genomics (Huntsville, Alabama) using the same primer pairs.

Genome sequencing and mining.—*Conoideocrella luteorostrata* ARSEF 14590 (CLUM14) was sequenced on the Illumina NextSeq 1000 platform at Marshall University Genomics Core Facility (Huntington, West Virginia). Illumina raw reads were assembled using SPAdes 3.15.2 and AAFTF 0.4.1 (Stajich and Palmer 2019). Unassembled reads are accessible through the National Center for Biotechnology Information (NCBI) Sequence Read Archive (SRA) via accession number SRR24939140, BioProject accession number PRJNA980380, and BioSample accession number SAMN35627742. This Whole Genome Shotgun project has been deposited at DNA DataBank of Japan (DDBJ)/European Nucleotide Archive (ENA)/GenBank under the accession JASWJB000000000. The version described in this paper is version JASWJB010000000. Assembly statistics for ARSEF 14590 can be found at: https://www.ncbi.nlm.nih.gov/datasets/genome/GCA_032433595.1/. To briefly summarize, genome size = 47.4 Mbp; coverage = 51.6×; L50 = 129; N50 = 107.1 kb; and GC content = 49. A BUSCO 5.4.4 (Manni et al. 2021) completeness assessment was 99.5% (1696 out of 1706 markers found) using the Ascomycota_odb10 data set with a duplication rate of 0.8%. Nucleotide sequences for *RPB1* (DNA-directed RNA polymerase II subunit 1), *RPB2* (DNA-directed RNA polymerase II subunit 2), *EF1-α* (elongation factor 1 alpha), *TUB2* (β-tubulin 2), and 18S were extracted from the ARSEF 14590 assembled genome using CL strains NHJ 12516 (EF468905, EF468946, and EF468994), NHJ 11343 (EF468801), and BCC 9617 (AY624237) reference sequences as BLAST alignment probes. These extracted sequences are deposited separately in NCBI Nucleotide database with accessions listed in TABLE 2. Sequences for TUB2 (OR500271) and 18S (OR492260) were not used in tree building but were deposited as well.

Alignments, model selection, and phylogenetic analyses.—Chromatograms for Sanger sequences were quality-checked using default parameters, clipped, and manually corrected in Geneious Prime (2023.1.2). Two data sets were compiled: (i) a 54-taxon, 4-locus (*RPB1, RPB2, EF1-α*, 28S) data set (hereafter referred to as the Clavicipitaceae data set) representing the diversity of the family based on previous phylogenetic studies (Johnson et al. 2009; Kepler et al. 2012; Mongkolsamrit et al. 2016) and (ii) a 38-taxon, 2-locus *Conoideocrella*-focused (*EF1-α*, 28S) data set (hereafter referred to as the CF data set) informed by the topology of the 4-locus analysis and previous phylogenetic studies (Artjariyasripong et al. 2001; Luangsa-ard et al. 2007; Saito et al. 2012; Urbina and Ahmed 2022). Both data sets included novel sequence data for CL ARSEF 14590. The CF data set also included 28S sequence data for five

Table 2. Species and isolates used in 54-taxon Clavicipitaceae phylogenetic analysis and their associated metadata.

Current name[a]	Authority	Synonyms	Strain	28S	*EF1-α*	*RPB1*	*RPB2*
Aciculosporium siamense	Mongkols., Noisrip. & Luangsa-ard, 2021	—	BCC 85384	MT743003	MT762148	MT762149	—
Aschersonia incrassata	Mains, 1959	—	PC 595	AY986909	AY986934	DQ000335	—
Atkinsonella texensis	(Diehl) Leuchtman & Clay, 1989	—	B6156	KQ062782	KQ062730	KQ062630	KQ062666
Balansia henningsiana	(Möller) Diehl, 1950	—	GAM 16112	AY489715	AY489610	AY489643	DQ522413
Claviceps fusiformis	Loveless, 1967	—	ATCC 26019	U17402	DQ522320	DQ522366	—
Claviceps paspali	F. Stevens & J.G. Hall, 1910	—	ATCC 13892	U47826	DQ522321	DQ522367	DQ522416
Claviceps purpurea	(Fr.) Tul., 1853	*Sphacelia segetum*	GAM 12885	AF543789	AF543778	AY489648	DQ522417
Commelinaceomyces aneilematis	(S. Ito) E. Tanaka, 2020	—	MAFF 246963	LC474617	LC474623	LC474626	LC474629
Conoideocrella luteorostrata	(Zimm.) D. Johnson, G.H. Sung, Hywel-Jones & Spatafora, 2008	*Torrubiella luteorostrata, Paecilomyces cinnamomeus*	ARSEF 14590/UM14	ON082755	OR500274	OR500272	OR500273
Conoideocrella luteorostrata	(Zimm.) D. Johnson, G.H. Sung, Hywel-Jones & Spatafora, 2008	*Torrubiella luteorostrata, Paecilomyces cinnamomeus*	NHJ 12516	EF468849	EF468800	EF468905	EF468946
Conoideocrella luteorostrata	(Zimm.) D. Johnson, G.H. Sung, Hywel-Jones & Spatafora, 2008	*Torrubiella luteorostrata, Paecilomyces cinnamomeus*	NHJ 11343	EF468850	EF468801	EF468906	—
Conoideocrella tenuis	(Petch) D. Johnson, G.H. Sung, Hywel-Jones & Spatafora, 2008	*Torrubiella tenuis*	NHJ 6293	EU369044	EU369029	EU369068	EU369087
Conoideocrella tenuis	(Petch) D. Johnson, G.H. Sung, Hywel-Jones & Spatafora, 2008	*Torrubiella tenuis*	NHJ 6791	EU369046	EU369028	EU369069	EU369089
Conoideocrella tenuis	(Petch) D. Johnson, G.H. Sung, Hywel-Jones & Spatafora, 2008	*Torrubiella tenuis*	NHJ 345.01	EU369045	EU369030	—	EU369088
Conoideocrella krungchingensis	Mongkols., Thanakitp. & Luangsa-ard, 2016	—	BCC 53667	KJ435071	KJ435100	—	—
Conoideocrella krungchingensis	Mongkols., Thanakitp. & Luangsa-ard, 2016	—	BCC 36100	KJ435080	KJ435097	—	—
Dussiella tuberiformis	(Berk. & Ravenel) Pat. ex Sacc., 1890	*Echinodothis tuberiformis*	JFW_NC2000	JQ257009	JQ257027	JQ257015	JQ257020
Epichloe typhina	(Pers.) Brockm., 1863	—	ATCC 56429	U17396	AF543777	AY489653	DQ522440
Helicocollum krabiensis	Luangsa-ard, Mongkols., Noisripoom & Thanakitp., 2017	—	BCC71372	KT222325	KT222340	KT222333	—
Hypocrella nectrioides	Thaxt., 1921	—	GJS 89–104	U47832	DQ522347	DQ522393	DQ522448
Hypocrella raciborskii	Zimmermann, 1901	*Aschersonia placenta*	BCC 7869	EF469074	EF469056	EF469085	EF469104
Hypocrella schizostachyi	Hennings, 1908	—	BCC 14123	DQ518771	DQ522346	DQ522392	DQ522447
Hypocrella siamensis	Hywel-Jones & Mongkols., 2009 Hywel-Jones & Mongkolsamrit, 2009	*Aschersonia badia*	BCC 8105	DQ518752	DQ522317	DQ522363	DQ522411
[*Hypocrella*] *hypoxylon* var. *piluliformis*	Berk. & M.A. Curtis, 1892	*Balansia pilulaeformis, Balansiopsis piluliformis, Dothidea piluliformis*	AEG 942	AF543788	DQ522319	DQ522365	DQ522414
Keithomyces neogunnii	(T.C. Wen & K.D. Hyde) Luangsa-ard, Thanakitpipattana & Samson, 2020	—	BUM_415	MH143828	MH143861	MH143876	MH143891
Marquandomyces marquandii	(Massee) Samson, Houbraken & Luangsa-ard, 2020	*Metarhizium marquandii, Paecilomyces marquandii*	CBS 127132	MT078857	MT078849	MT078865	MT078922
Metapochonia goniodes	(Drechsler) Kepler, S.A. Rehner & Humber, 2014	*Pochonia gonioides, Verticillium gonioides*	CBS 891.72	AF339550	DQ522354	DQ522401	DQ522458
Metarhizium album	Petch, 1931	—	ARSEF 2082	DQ518775	DQ522352	DQ522398	DQ522452

(*Continued*)

Table 2. (Continued).

Current name[a]	Authority	Synonyms	Strain	28S	*EF1-α*	*RPB1*	*RPB2*
Metarhizium anisopliae	(Metschn.) Sorokin, 1883	*Isaria anisopliae, Penicillium anisopliae*	ARSEF 3145	AF339530	AF543774	DQ522399	DQ522453
Metarhizium flavoviride	W. Gams & Rozsypal, 1973	—	ARSEF 2037	AF339531	DQ522353	DQ522400	DQ522454
Metarhizium guizhouense	Q.T. Chen & H.L. Guo, 1986	*Cordyceps taii, Metacordyceps taii, Metarhizium taii*	ARSEF 5714	AF543787	AF543775	DQ522383	DQ522434
Moelleriella epiphylla	(Massee) P. Chaverri & K.T. Hodge, 2008	*Hypocrella epiphylla*	PC386	EU392582	EU392659	EU392710	—
Morakotia fusca	Mongkols., Noisrip., Khons., Thanakitp. & Luangsa-ard, 2021	—	BCC 79272	KY794861	KY794856	KY794865	—
Myriogenospora atramentosa	(Berk. & M.A. Curtis) Diehl, 1950	—	AEG9632	AY489733	AY489628	AY489665	DQ522455
Nigelia martialis	Luangsa-ard & Thanakitp., 2017	*Metacordyceps martialis, Metarhizium martialis*	BUM_713	MH143824	MH143858	MH143873	MH143888
Orbiocrella petchii	(Hywel-Jones) D. Johnson, G.H. Sung, Hywel-Jones & Spatafora, 2008	*Torrubiella petchii*	NHJ 5318	EU369040	EU369021	EU369062	EU369080
Orbiocrella petchii	(Hywel-Jones) D. Johnson, G.H. Sung, Hywel-Jones & Spatafora, 2008	*Torrubiella petchii*	NHJ 6209	EU369039	EU369023	EU369061	EU369081
Orbiocrella petchii	(Hywel-Jones) D. Johnson, G.H. Sung, Hywel-Jones & Spatafora, 2008	*Torrubiella petchii*	NHJ 6240	EU369038	EU369022	EU369060	EU369082
Papiliomyces sp. YZ-2021a	N/A	—	YC20061404	MZ702102	MZ955881	MZ955877	OM419144
Parametarhizium hingganense	S. Gao, W. Meng, Li Xiang Zhang, Q. Yue, L. J. Xu, 2021	—	SGSF355	MN061635	MN065770	MN917170	MT939494
Periglandula ipomoeae	U. Steiner, Leistner & Schardl, 2011	—	IasaF13	AFRD01000776	AFRD01000133	AFRD01000003	AFRD01000102
Pochonia chlamydosporia	(Goddard) Zare & W. Gams, 2001	*Cordyceps chlamydosporia, Diheterospora chlamydosporia, Verticillium chlamydosporium* var. *chlamydosporium, Verticillium catenulatum, Metacordyceps chlamydosporia*	CBS 101244	DQ518758	DQ522327	DQ522372	DQ522424
Pochonia cordycepisociata	H. Huang, M. Wang & L. Cai, 2015	—	CGMCC 317365	KM263573	KM263584	KM263576	KM263579
Pseudogibellula formicarum	(Mains) Samson & H.C. Evans, 1973	—	BCC 84257	MT512653	MT533480	MT533473	—
Purpureomyces pyriformis	Luangsa-ard, Noisripoom, Himaman, Mongkolsamrit, Thanakitpipattana & Samson, 2020	—	BCC 85348	MN781871	MN781728	MN781773	MN781820
Regiocrella camerunensis	P. Chaverri & H.C. Evans, 2006	—	ARSEF 7682	DQ118735	DQ118743	DQ127234	—
Rotiferophthora angustispora	(G.L. Barron) G.L. Barron, 1991	—	CBS 101437	AF339535	AF543776	DQ522402	DQ522460
Samuelsia chalalensis	P. Chaverri & K.T. Hodge, 2008	—	PC560	EU39263	EU392691	EU392743	—
Shimizuomyces paradoxus	Kobayasi, 1981	—	EFCC 6279	EF469084	EF469071	EF469100	EF469117
Tolypocladium ophioglossoides	(Ehrh. ex J.F. Gmel.) Quandt, Kepler & Spatafora, 2014	*Cordyceps ophioglossoides, Elaphocordyceps ophioglossoides*	OSC 106405	AY489723	AY489618	AY489652	DQ522429
[Torrubiella] hemipterigena	Petch, 1931	*Verticillium hemipterigenum*	Allpaths-LG	CDHN01000016	CDHN01000003	CDHN01000002	CDHN01000003
Ustilaginoidea virens	(Cooke) Takah., 1896	*Claviceps virens, Villosiclava virens*	ATCC 16180	—	JQ257026	JQ257014	JQ257019
[Verticillium] epiphytum	Hansford, 1943	*Verticillium epiphytum*	CBS 384.81	AF339547	DQ522361	DQ522409	DQ522469
Yosiokobayasia kusanaginensis	(Kobayasi & Shimizu) Samson, Luangsa-ard & Thanakipipattana, 2020	*Metacordyceps kusanaginensis, Metarhizium kusanaginense*	TNS-F 18494	JF415972	JF416014	JN049890	—

Note. — denotes no data available.
[a]Square brackets ([]) around a genus indicates that the name awaits appropriate action by the research community to be transferred to another genus as indicated in NCBI Taxonomy Browser.

additional CL strains. Strain tables for each analysis are available in TABLE 2 (Clavicipitaceae data set) and TABLE 3 (*Conoideocrella*-focused data set).

Each locus was aligned separately using MAFFT (Katoh & Standley 2013) on the GUIDANCE2 server (http://guidance.tau.ac.il/; Landan & Graur 2008; Sela et al. 2015), and individual residues with GUIDANCE scores <0.5 were masked. An intron in *RPB1* (positions 118 to 247) was deleted. The best nucleotide substitution models for each locus were selected by ModelTest in MEGA11 (Tamura et al. 2021), using the corrected Akaike information criterion (AlCc) score. GTR+G was determined to be the optimal model for all analyses.

Single-locus alignments and concatenated alignments for both data sets were all used for tree building. Maximum likelihood (ML) trees were created using RAxML 8.2.12 (Stamatakis 2014) with 1000 bootstrap replicates. Bayesian inference (BI) trees were generated using MrBayes 3.2.7a (Ronquist et al. 2012), using 1 million generations except for the 28S Clavicipitaceae analysis, which required 3.4 million generations for the standard deviation of split frequencies to fall below 0.01. For BI analyses, one cold chain and three heated chains were used for each run, and the first 25% of generations were discarded as burn-in. Finally, runs were checked for convergence in Tracer 1.7.1 (Rambaut et al. 2018). For concatenated data sets, the ML tree was used for topology and branch lengths and was annotated with BI support values where topology was in agreement. Trees were viewed and prepared for publication using FigTree 1.4.4 (Rambaut et al. 2018) and Inkscape 0.92.2 https://www.inkscape.org/). Resulting trees, alignments, and other data are available on GitHub: https://github.com/HanaBarrett/EHS-CL-Analysis.

RESULTS

Morphological investigation.—An emergent fungal epizootic of *Conoideocrella luteorostrata* (CL) was found impacting the first instar crawler stage of elongate hemlock scale (EHS) on planted Fraser fir trees across three Christmas tree farms in Ashe County, North Carolina, in

Table 3. Species and isolates used in 38-taxon *Conoideocrella*-focused phylogenetic analysis and their associated metadata.

Current name	Strain	Location[a]	Host order	Host family	Host species	28S	*EF1-α*
Conoideocrella krungchingensis	BCC 36100	Thailand	Hemiptera	Diaspididae	—	KJ435080	KJ435097
Conoideocrella krungchingensis	BCC 36101	Thailand	Hemiptera	Diaspididae	—	KJ435081	KJ435098
Conoideocrella krungchingensis	BCC 53666	Thailand	Hemiptera	Diaspididae	—	KJ435070	KJ435099
Conoideocrella luteorostrata	555	Thailand	—	—	—	AF327380	—
Conoideocrella luteorostrata	2692	Thailand	—	—	—	AF327388	—
Conoideocrella luteorostrata	Kyoto-32	Japan	Hemiptera	Aleyrodidae	*Aleurocanthus camelliae*	—	AB663122
Conoideocrella luteorostrata	Mie-2	Japan	Hemiptera	Aleyrodidae	*Aleurocanthus camelliae*	—	AB663130
Conoideocrella luteorostrata	Shiga-2	Japan	Hemiptera	Aleyrodidae	*Aleurocanthus camelliae*	—	AB663124
Conoideocrella luteorostrata	Shiga-4	Japan	Hemiptera	Aleyrodidae	*Aleurocanthus camelliae*	—	AB663125
Conoideocrella luteorostrata	NHJ 12516	Thailand	Hemiptera	—	—	EF468849	EF468800
Conoideocrella luteorostrata	NHJ 11343	Thailand	Hemiptera	—	—	EF468850	EF468801
Conoideocrella luteorostrata	BCC 9617	Thailand	Hemiptera	—	—	KJ435068	KJ435086
Conoideocrella luteorostrata	BCC 14222	Thailand	—	—	—	KJ435069	KJ435087
Conoideocrella luteorostrata	BCC 53671	Thailand	—	—	—	KJ435072	KJ435088
Conoideocrella luteorostrata	BCC 53673	Thailand	—	—	—	KJ435074	KJ435090
Conoideocrella luteorostrata	BCC 53675	Thailand	—	—	—	KJ435075	KJ435091
Conoideocrella luteorostrata	BCC 53677	Thailand	—	—	—	KJ435077	KJ435092
Conoideocrella luteorostrata	2020–105941	USA	Hemiptera	Diaspididae	*Fiorinia externa*	MW419877	—
Conoideocrella luteorostrata	UM11	USA	Hemiptera	Diaspididae	*Fiorinia externa*	ON082754	—
Conoideocrella luteorostrata	ARSEF 14590/UM14	USA	Hemiptera	Diaspididae	*Fiorinia externa*	ON082755	OR500274
Conoideocrella luteorostrata	VF11	USA	Hemiptera	Diaspididae	*Fiorinia externa*	ON082756	—
Conoideocrella luteorostrata	VF41	USA	Hemiptera	Diaspididae	*Fiorinia externa*	ON082757	—
Conoideocrella luteorostrata	VF42	USA	Hemiptera	Diaspididae	*Fiorinia externa*	ON082759	—
Conoideocrella luteorostrata	BAF11	USA	Hemiptera	Diaspididae	*Fiorinia externa*	ON082753	—
Conoideocrella tenuis	BCC 44534	Thailand	Hemiptera	—	—	MG198773	MG230541
Conoideocrella tenuis	NHJ 345.01	—	Hemiptera	—	—	EU369045	EU369030
Conoideocrella tenuis	BCC 53676	Thailand	—	—	—	KJ435076	KJ435096
Conoideocrella tenuis	BCC 2206	Thailand	Hemiptera	—	—	KJ435078	KJ435095
Conoideocrella tenuis	BCC 2129	Thailand	Hemiptera	—	—	KJ435083	KJ435094
Conoideocrella tenuis	BCC 1411	Thailand	—	—	—	KJ435079	KJ435093
Conoideocrella tenuis	NHJ 6791	Japan	Hemiptera	—	—	EU369046	EU369028
Conoideocrella tenuis	NHJ 6293	Japan	Hemiptera	—	—	EU369044	EU369029
Dussiella tuberiformis	JFW_NC2000/MYA-2810	USA	Hemiptera	—	—	JQ257009	JQ257027
Dussiella tuberiformis	B351/ATCC 201937	—	—	—	—	U68126	—
Dussiella tuberiformis	JFW_AL	USA	—	—	—	U57083	—
Orbiocrella petchii	NHJ 5318	—	Hemiptera	—	—	EU369040	EU369021
Orbiocrella petchii	NHJ 6209	Thailand	Hemiptera	—	—	EU369039	EU369023
Orbiocrella petchii	NHJ 6240	Thailand	Hemiptera	—	—	—	EU369022

[a]THA, Thailand; JPN, Japan; and USA, United State of America. — denotes no data available.

the summer of 2020. Hundreds of thousands of mycosed individuals were observed across the three North Carolina sampling locations, with the heaviest infections occurring at VF, followed by UM then BAF (FIG. 1A–B). No mycosed EHS were found in Virginia at MRO, despite the presence of EHS at this location. Neither healthy nor mycosed EHS were recovered from MR, although healthy Fraser fir needles were sampled. At VF, CL was also observed and isolated from one adult female EHS. Infected EHS were identifiable by the distinct orange mat of hyphae (stromata) covering the nymph cadavers. Mycosed EHS were abundant, with multiple infected cadavers on each affected needle (FIG. 1A).

Morphological studies were undertaken to compare four CL strains isolated from two sampling sites (UM, VF) in North Carolina with previously reported measurements for this species (Samson 1974; Hywel-Jones 1993; Saito et al. 2012), other *Conoideocrella* species (Hywel-Jones 1993; Mongkolsamrit et al. 2016), and *Dussiella tuberiformis* (Atkinson 1891).

Newly established CL colonies were of a distinct tannish orange color that gradually changed to cinnamon-brown on PDA+ST. After about a week of growth, CL colonies begin to secrete a yellow soluble pigment (FIG. 1G–H), eventually turning a purplish red as the cultures aged (FIG. 1F). This was apparent in both the agar and as guttation droplets atop the older inner mycelium (FIG. 1G, right panel). These droplets were also observed atop CL colonies on Czapek-Dox agar (photos not shown). After several weeks, colonies were covered with green conidia (FIG. 1E–F).

Subsequent microscopic examination of these four CL strains in lactic acid (± cotton blue) confirmed the presence of whorled (verticillate) conidiophores with flask-shaped phialides and hyaline, smooth-walled, aseptate conidia with acute ends (FIG. 1I–L). As cultures aged, basipetal chains of conidia were observed, resulting in a characteristic powdery, green appearance (FIG. 1F, J). Based on the taxonomic keys of Samson (1974) and subsequent descriptions from Saito et al. (2012), the fungus aligned morphologically with *Paecilomyces cinnamomeus*, the asexual state of CL.

Conidia averaged 6.9 (5.4–8.0) µm in length × 2.6 (2.0–3.3) µm in width across the four examined CL strains (TABLE 4). Among them, mean spore lengths and widths were significantly larger ($P < 0.05$) for two strains. ARSEF 14590 (mean 7.4 × 2.5 µm) and VF11 (mean 7.2 × 2.8 µm) had significantly larger mean conidial lengths ($P < 0.05$) compared with UM11 (mean 6.6 × 2.7 µm) and VF41 (mean 6.5 × 2.4 µm) (FIG. 2). For conidial width, VF11 (7.2 × 2.8 µm) has significantly larger spore width ($P < 0.05$) compared with VF41 (6.5 × 2.4 µm), but neither was significantly different from UM11 or ARSEF 14590. Overall, our results suggest that there is considerable variation in conidial length among our isolates. However, the conidial lengths for all four strains fell within the ranges reported by Hywel-Jones (1993), Samson (1974), and Saito et al. (2012). Additionally, all four CL strains had conidial widths that overlapped with Hywel-Jones (1993). UM11 and VF41 also had conidial widths that overlapped with Saito et al. (2012) and VF41 overlapped with Samson (1974) (FIG. 2). Raw spore measurements are available in SUPPLEMENTARY TABLE 5. Nearly all strains examined, including measurements reported from aforementioned taxonomic papers, overlapped partially with the conidial measurements reported for a *Hirsutella*-like asexual state of CK (Mongkolsamrit et al. 2016), which covered a much larger range of both length and width. However, unlike CK, CL conidia were exclusively aseptate. Measurements for *Dussiella tuberiformis* were distinct from all CL strains, with the exception of minimal overlap in spore length in ranges reported by Hywel-Jones (1993) (FIG. 2). Ascospore measurements were not compared, as the sexual stage was not observed on mycosed EHS during this study: perithecia have never been reported from

Table 4. Ascospore and conidial measurements for *Conoideocrella* species and *Dussiella tuberiformis* with associated references.

Species ID	Ascospores (µm)	Asexual state	Conidia (µm)	N (isolates/spores)[a]	Reference
Conoideocrella luteorostrata	460–590 × 1.5–2	*Paecilomyces cinnamomeus*	6.5–8.3 × 2.0–3.6	—	Hywel-Jones 1993
	—	*Paecilomyces cinnamomeus*	5.2–7.5 × 1.7–2.5	—	Samson 1974
	—	*Paecilomyces cinnamomeus*	5.2–7.6 × 2.3–2.6	12/600	Saito et al. 2012
	—	*Paecilomyces cinnamomeus*	6.2 (4.5–8.0) × 1.9 (1.8–2.9)	4/100	This study
Conoideocrella tenuis	380–500 × 1.5–2	Unknown	—	—	Hywel-Jones 1993
Conoideocrella krungchingensis	(80–)110–150 × 1.5–2.5	*Hirsutella*-like	8–15 × 2–4	—	Mongkolsamrit et al. 2016
Dussiella tuberiformis	450–750 × 14	Sphacelia-like	7–10 × 3.5–4	—	Atkinson 1891

Note. — denotes no data available.
[a]Denotes total isolates used and total spores measured across all isolates.

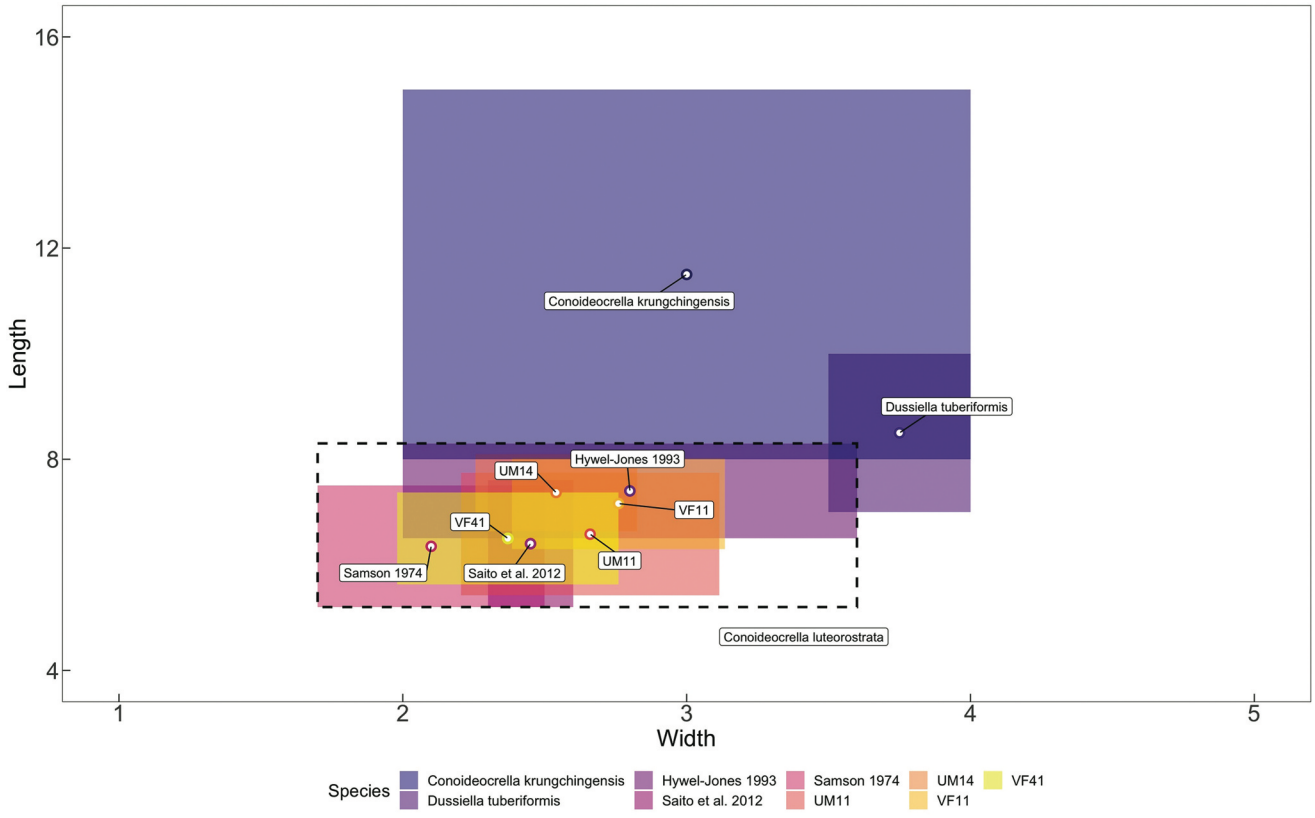

Figure 2. Primary conidial length and width measurements (µm) for strains from North Carolina overlaid atop measurements previously reported for *C. luteorostrata* (inside black dashed line), *C. krungchingensis*, and *D. tuberiformis*. Mean values are denoted by a circle. For CL measurements, names following colored box denotes paper from which the measurements were pulled. All other CL strain data were generated as part of this study. Measurements also available in TABLE 4 and SUPPLEMENTARY TABLE 5.

U.S. hemipterans infected with CL, although herbarium specimens of CL from AL, FL, LA, and MS have not been examined for such fruiting bodies.

A *Hirsutella*-like asexual state with paired aseptate to uniseptate conidia formed on simple conidiophores was also observed for ARSEF 14590 after 14 days (FIG. 3). A mucous sheath was visible immediately surrounding the paired fusiform to slightly curved conidia atop each conidiophore, as evidenced by the absence of mountant infiltration (FIG. 3B–E). Sporulation was sparse, conidia stuck together and were and intermixed with conidiophores of the *Paecilomyces*-like synanamorph, which limited the ability to report measurements specifically for this synanamorph except for uniseptate conidia, which were completely absent from the *Paecilomyces*-like colonies examined on standard growth media and conditions (FIG. 1I–L). A single uniseptate spore in mucous sheath and still attached to its conidiophore measured 8.9 × 2.0 µm, exceeding the length of all previously reported and measured conidia across all CL strains. No propagules or blastospores were observed in liquid culture.

For temperature growth assays, our two examined CL strains grew optimally around 22 C, with an estimated radial growth rate of 0.95 mm/day on PDA+ST, but neither actively grew at 10 or 30 C. Because some plates developed satellite colonies over the course of the first 2-week period, only four plates were available per isolate per temperature, with the exception of BAF45, which had three at 10 C and five at 22 C. Both strains were able to resume normal growth when returned to 22 C after 7 days' exposure to either temperature.

Culture-based survey of fir needles for CL.—A total of 81 fungal isolates representing 31 fungal morphotypes were recovered from 60 Fraser fir needles (48 living and 12 dead) sampled across five sampling locations. In total, 24 total and 18 unique morphotypes were recovered from living fir needles, and 14 total morphotypes were recovered from EHS+CL+ trees, of which 6 morphotypes were absent from EHS+CL− and EHS−CL− trees. However, none of the 31 recovered morphotypes, including the 6 unique morphotypes associated with CL+ trees, shared any characteristics that distinguish CL/PC.

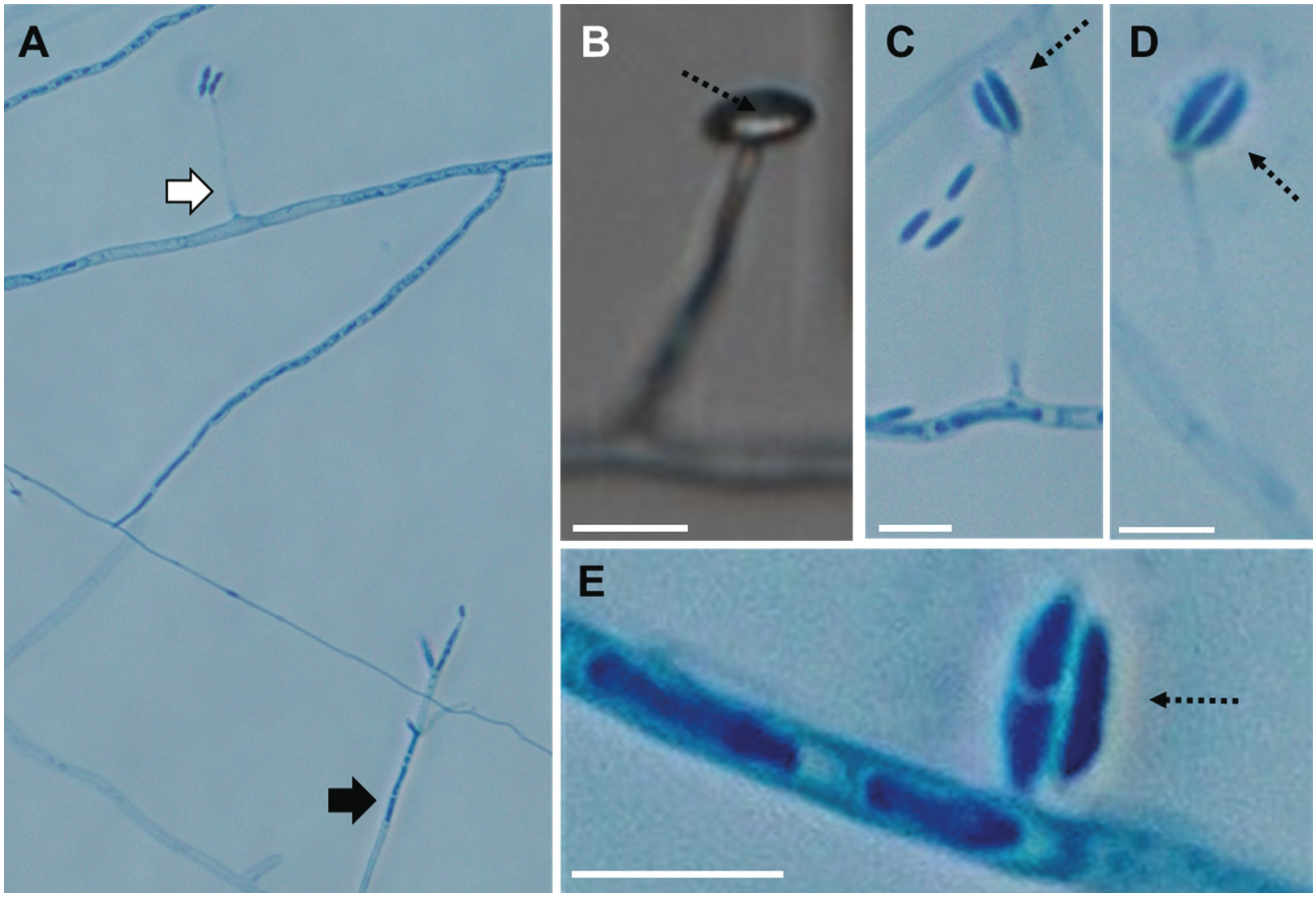

Figure 3. Conidiophores and conidia of *Hirsutella*-like asexual stage of *C. luteorostrata* strain ARSEF 14590/CLUM14 sporulating beneath glass slipcovers on stab-inoculated PDA slides. A. Both *Paecilomyces*-like (black arrow) and *Hirsutella*-like (white arrow) asexual states co-occurring on the same slide. B–D. Conidiophores showing paired terminal fusiform conidia with mucous sheath (dashed arrows show areas absent of mountant infiltration). E. A transversely septate and aseptate conidium still paired within a mucous sheath detached from the conidiophore. Bars: B–E = 10 µm.

Superficial arthropod survey for CL-infected arthropods.—Seventy nonsessile arthropods were collected from our CL+ branch samples (SUPPLEMENTARY TABLE 4). No outward fungal infections were observed in these arthropods. The most common arthropod encountered was the beetle *Cybocephalus nipponicus*, a known predator of EHS, which was collected from VF and BAF: both of these sites were not being managed for production during collection, and, as such, both hosted denser EHS populations. Two parasitoid wasps were also collected: one of these was observed ovipositing into an EHS adult female prior to collection. We identified these parasitoid wasps as *Encarsia citrina*, a known parasitoid of EHS. EHS-parasitoid wasps were also observed developing within the tests of collected female elongate hemlock scales under microscopic examination. None of these natural enemies of EHS or other arthropods exhibited outward fungal infections. No isolations were attempted from these outwardly asymptomatic insects.

Laboratory pathogenicity bioassays.—In our first bioassay, EHS-infested needles were treated with a CL suspension and crawlers were allowed to emerge over the course of the bioassay. EHS are known to have continuous emergence across the season, and this was observed for the duration of both bioassays. This presented challenges for counting moving crawlers when numbers rose above ~20 individuals, and it also resulted in continuous exposure to CL: some crawlers were initially infected on day 0, whereas others were infected on day 13 (FIG. 4A). This continuous emergence resulted in percent survival increasing on some days (FIG. 4A). Crawler vitality was recorded daily for both treatments for Kaplan-Meier survival analysis. CL-treated EHS and controls were significantly different (log-rank test, $P = 0.03$). The survival curve (FIG. 4B) documenting daily percent survival in this bioassay revealed lower survival in the CL treatment late in our bioassay (i.e., days 10–13), but continuous crawler emergence prevented survival from falling below 50%.

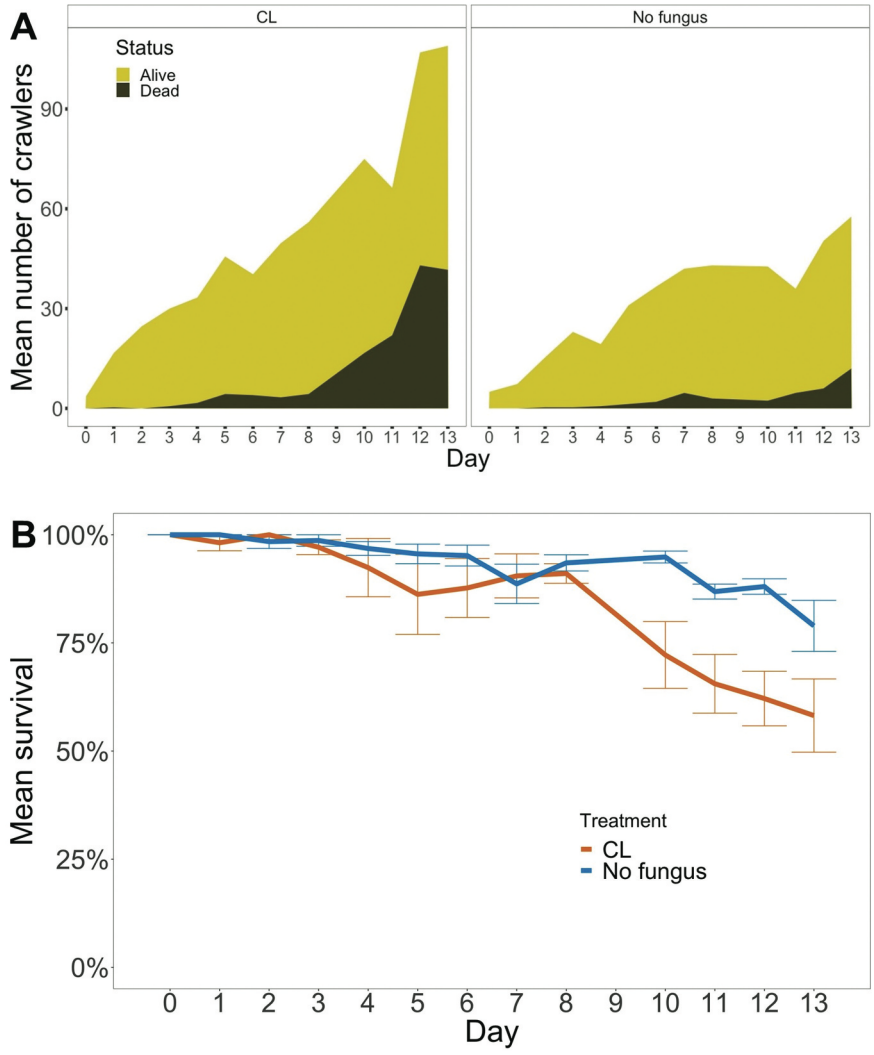

Figure 4. A. Crawler emergence by treatment over the course of our bioassay. Mean total crawlers (across 3 replicates) are represented by the yellow area, whereas mean dead crawlers are represented in black. B. Calculated percent survival for each treatment.

In our second bioassay, crawlers were introduced onto CL-treated branchlets and cadavers were collected 2 weeks after exposure. An asymptomatic crawler, a treated crawler exhibiting melanization (insect immune response to infection) and fungal outgrowth, and a cadaver with visible conidiophores with paired to whorled phialides typical of CL can be seen in FIG. 5A–C. CL was isolated from three of five surface-sterilized crawler cadavers and identified through colony and conidial morphology and Sanger sequencing of the ITS region. CL was not isolated from any of three surface-sterilized crawlers randomly sampled from the control group.

CL molecular identification.—BLASTn searches against NCBI GenBank using our isolates as queries revealed that three of our seven strains (ARSEF 14590, UM11, and VF11) were 100% identical to two CL ITS sequences (MW419875, MW419876) that were recently deposited from mycosed EHS in North Carolina (independent of our study; Urbina and Ahmed 2022) and one CL ITS sequence (AB649298) from a mycosed whitefly in Japan in 2009 (Saito et al. 2012). To identify the degree of sequence similarity among the seven novel CL isolates, pairwise BLASTn searches were conducted and revealed sequence similarity ranging from 99.81% to 100% across all ITS sequences (deposited under GenBank accessions ON081993–ON081999). BLASTn searches were also conducted for ARSEF 14590 β-tubulin 2 (BTUB) and 18S sequences, revealing 99.4% sequence similarity to TUB2 sequences deposited for CL Kyoto-26 (AB663108) and Shiga-4 (AB663113) from Japan and 100% sequence similarity to 18S sequences deposited for CL NHJ 11343 (EF468995) and NHJ 12516 (EF468994) from Thailand.

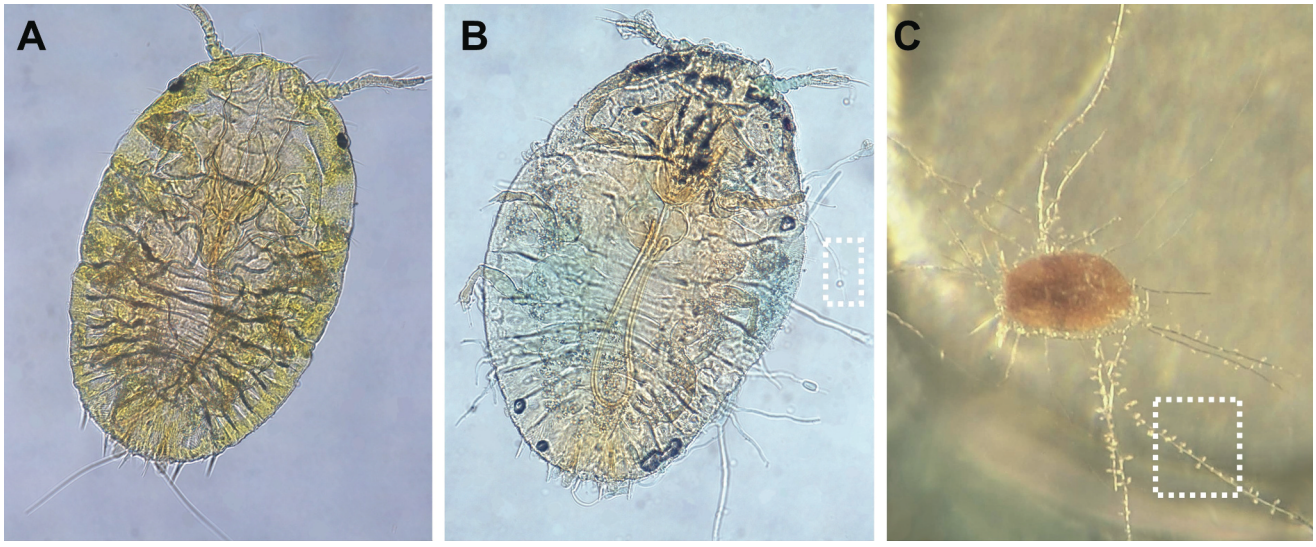

Figure 5. A–B. Asymptomatic EHS crawler from control treatment at 40× magnification (A) compared with crawler from CL+ treatment (40×) exhibiting melanization, which was associated with infection (B). C. Dead mycosed crawler with *C. luteorostrata* outgrowth under dissecting microscope. Dashed white boxes in B and C emphasize fungal growth with obvious paired to whorled conidiophores characteristic of CL seen in C.

***Phylogenetic analysis of* Conoideocrella *spp. and closely allied fungi.*—**To examine phylogenetic relationships among diverse members of the Clavicipitaceae, the three formally recognized *Conoideocrella* species, and multiple CL strains including our seven strains from North Carolina, phylogenetic analyses were conducted for a 54-taxon, 4-locus Clavicipitaceae data set and separately for a 38-taxon, 2-locus *Conoideocrella*-focused (CF) data set representing the diversity of strains in *Conoideocrella* and closely allied genera. Single-locus and combined data sets were analyzed for both data sets using two methods of phylogenetic inference for a total of 10 analyses for the Clavicipitaceae data set and 6 analyses for the CF data set.

For the Clavicipitaceae data set, both ML and BI resolved CL as a strongly supported (>94% bootstrap support/>0.99 posterior probability) monophyletic lineage for all single-locus (*RPB1, RPB2, EF1-α*, and 28S) analyses and in the concatenated 4-locus analysis (FIG. 6; SUPPLEMENTARY FIGS. 1–4). CT also received strong support both in the *RPB1* and *RPB2* single-locus analyses (SUPPLEMENTARY FIGS. 3–4) and the combined analysis (FIG. 6). CT received moderate (71%/0.98) support in the *EF1-α* analysis (SUPPLEMENTARY FIG. 1). *RPB1* and *RPB2* sequence data were not available for CK, but the species was strongly supported (100%/1.0) in the 28S, *EF1-α*, and combined analyses (SUPPLEMENTARY FIGS. 1–2).

Dussiella tuberiformis formed a well-supported clade with CL and CT in the *RPB1, RPB2*, and concatenated analyses for the Clavicipitaceae data set (FIG. 6; SUPPLEMENTARY FIGS. 3–4). However, *EF1-α* and 28S single-locus trees did not resolve congruent topologies (SUPPLEMENTARY FIGS. 1–2). In both trees, the relationships among CT, CL, CK, and DT could not be resolved, with little to no support in the backbone of both trees. Regardless, no tree containing both CK and DT supports the monophyly of *Conoideocrella*. In the concatenated analysis, DT emerges between the clade that contains CL and CT and the CK clade (FIG. 6).

Orbiocrella petchii (OP) formed a well-supported, genealogically exclusive lineage across all analyses, with the exception of the 28S analysis, which revealed OP to be paraphyletic, with one strain grouping with CT (SUPPLEMENTARY FIG. 2). OP formed a moderately to well-supported clade with CL, CT, and DT in the *RPB1, RPB2*, and concatenated trees (FIG. 6; SUPPLEMENTARY FIGS. 3–4). However, *EF1-α* and 28S single-locus trees were incongruent: placement of OP occurred elsewhere as a single clade (*EF1-α*; SUPPLEMENTARY FIG. 1) or as paraphyletic (28S; SUPPLEMENTARY FIG. 2).

For the Clavicipitaceae data set, *RPB1* and *RPB2* supported the largest number of nodes at ≥70% ML/ >0.70 BI (n = 23 and 18, respectively). By contrast, 28S was the least informative with 9 supported nodes (SUPPLEMENTARY FIG. 2). Low support in the backbone of all single-locus trees emphasizes the need for multilocus phylogenetic studies. Given the paucity of publicly available *Conoideocrella* sequence

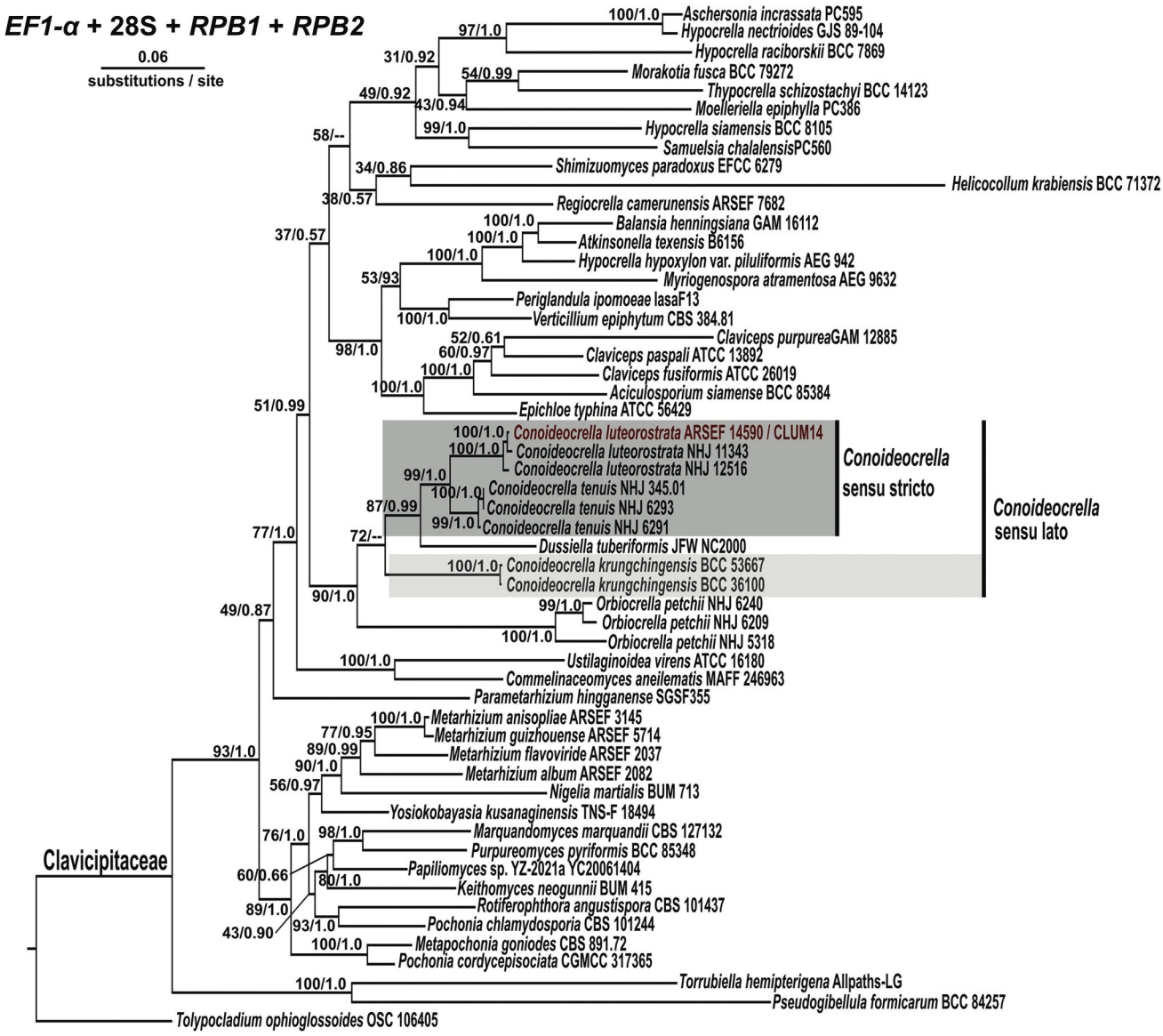

Figure 6. Concatenated phylogenetic tree for the Clavicipitaceae data set (28S + *EF1-α* + *RPB1* + *RPB2*). Topology and branch lengths shown are from the ML analysis. Bootstrap support and posterior probabilities are indicated for each node supported in the ML analysis (ML/BI). Strain metadata including GenBank accession numbers are listed in TABLE 2

data for *RPB1* and *RPB2* (n = 5/locus including ARSEF 14590), only 28S and *EF1-α* were advanced for the *Conoideocrella*-focused (CF) 38-taxon data set. The results from the Clavicipitaceae data set also helped inform appropriate ingroup and outgroup taxa for the CF data set, with *Conoideocrella* and *Dussiella* serving as the ingroup and *Orbiocrella* as the outgroup.

For the CF data set, both ML and BI resolved CL as a strongly supported (>95%/>0.99) monophyletic lineage for both the single-locus analyses (*EF1-α* and 28S) and the concatenated analysis (FIG. 7). The *EF1-α* single-locus analysis further resolved one well-supported (89%/0.87) clade within CL containing our isolate (ARSEF 14590), four Japanese strains from whitefly, and three strains from Thailand (FIG. 7A). The 28S analysis resolved a moderately supported (69%/0.84) clade in CL that contained ARSEF 14590, the same three strains from Thailand, and additional strains not present in the *EF1-α* tree due to missing data, including more North Carolina strains from this study and strain 2020-105941, an independently acquired strain from elongate hemlock scale in Virginia (FIG. 7B). The Japanese strains from whitefly were also excluded from the 28S analysis, as no sequence data were available. Any fine-level resolution among CL isolates supported by single-locus trees was absent in the concatenated tree (FIG. 7C).

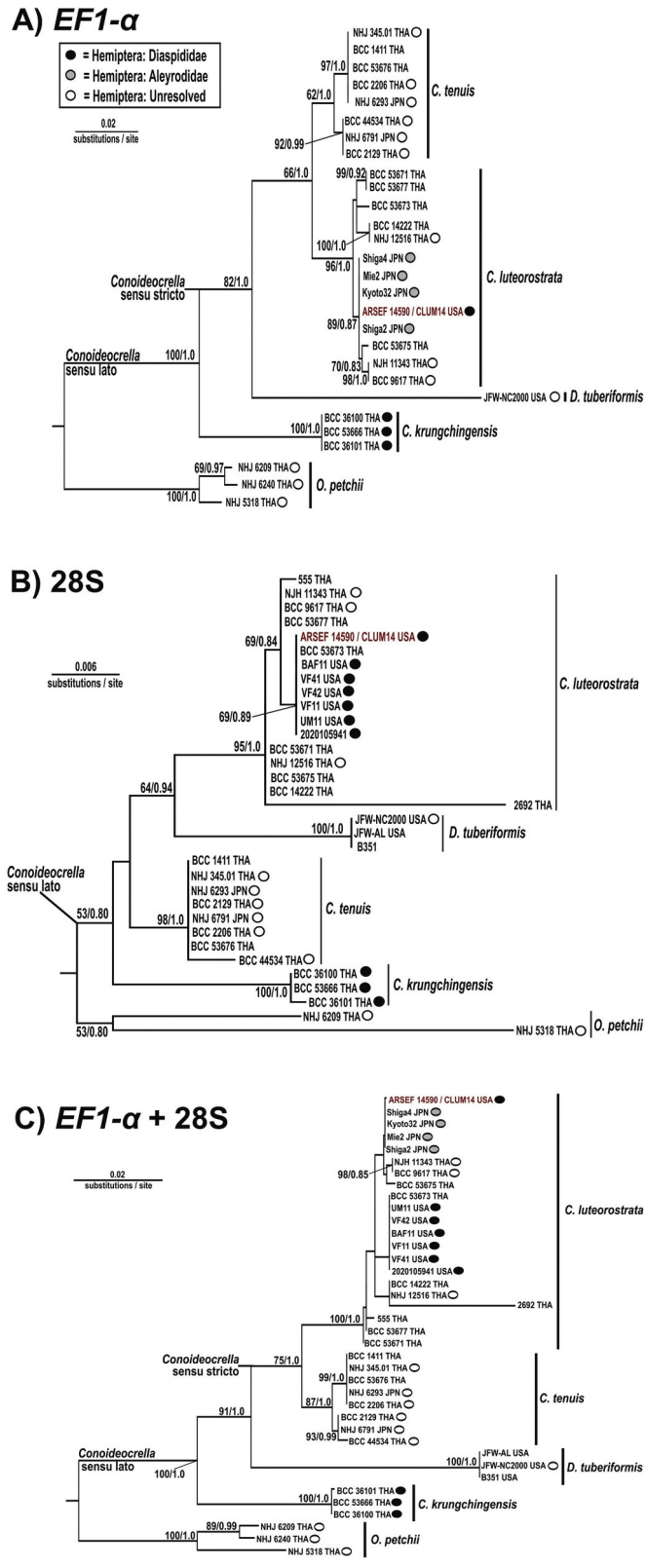

Figure 7. Phylogenetic trees for *EF1-α* (A), 28S (B), and concatenated (C) *Conoideocrella*-focused data sets. Topology and branch lengths shown are from the ML analysis. Bootstrap support and posterior probabilities are indicated for each node supported at or above 50% in the ML analysis (ML/BI). Country of origin and insect host associations are denoted for all taxa where data are available with key for host taxa in tree 7A. Strain metadata including GenBank accession numbers are listed in TABLE 3.

CT and CK also formed well-supported genealogically exclusive lineages across all analyses except for CT in the *EF1-α* analysis, which received only moderate (62%/1.0) support (FIG. 7). Despite the moderate support for CT, *EF1-α* and concatenated analyses further resolved two clades within CT, both containing strains from Thailand and Japan (FIG. 7A, C).

Despite the strong support for all three individual species from both methods of phylogenetic inference, *Conoideocrella* is polyphyletic (FIG. 7). *Dussiella tuberiformis* formed a strongly supported genealogically exclusive lineage either sister to CL (28S: 64%/0.94) or sister to a clade containing both CL and CT (82%/1.0 for *EF1-α* and 91%/1.0 for the concatenated tree). In both the single-locus and concatenated trees, CK fell outside the clade containing CL, CT, and *D. tuberiformis* (FIG. 7).

For the CF data set, *EF1-α* had a higher number of supported nodes (12 nodes at ≥70%/0.7) compared with 28S (4 nodes at ≥70%/0.7). The combining of *EF1-α* and 28S data sets weakens intraspecies resolution. Based on the results of the single-locus and 2-locus data sets, *EF1-α* alone appears to be the most robust candidate locus for intraspecies-level resolution for both CL and CT, providing strong support along the backbone of the phylogeny.

DISCUSSION

Our recent discovery of a naturally occurring epizootic of the anamorphic state of *C. luteorostrata* on elongate hemlock scale in North Carolina Christmas tree farms suggests potential for this fungus as a biocontrol agent. This exotic pest, although economically significant, does not currently have a commercially available fungal biocontrol option for tree farms, where it primarily infests fir. As with many armored scale insects, chemical insecticides may be ineffective due to varying nontarget effects on natural predators, insufficient spray coverage due to tree size or timing of application, and/or diminished efficacy due to natural resistance of adult females (Sidebottom 2016). A 2022 survey by Urbina and Ahmed supports the relatively recent expansion of this fungus across EHS populations impacting Christmas tree production in Virginia, North Carolina, and Michigan, but more expansive surveys across other plant and insect hosts are needed, especially given the numerous historical reports of anamorphic CL from whiteflies, soft scales, and armored scales, including citrus whitefly across at least four southeastern U.S. states between 1913 and 1939 (TABLE 1). CL co-occurs with *Dussiella tuberiformis* and at least two other Clavicipitaceae whitefly entomopathogens, *Aschersonia aleyrodis* and *A. goldiana* (Fasulo and Weems 1999; Martini et al. 2022), across much of the same geographic area. Dubious iNaturalist observations, coupled with the limited host data for these species, add further uncertainty to host and species boundaries for these fungi across the southeastern U.S.

In this study, we expanded on the current understanding of the U.S. population of CL with a robust phylogenetic and morphological investigation of our strains and compared them with CL, other *Conoideocrella* spp., and DT strains from the peer-reviewed literature. Our work confirmed that CL strains recovered from North Carolina (including strains independently isolated by Urbina and Ahmed (2022)) form a well-supported clade within CL that included whitefly strains from Japan and strains from Thailand (FIG. 7A). Our morphological data overlap considerably with all previously reported measurements for CL, with the exception of conidial widths reported by Hywel-Jones (1993), which cover a wider range of measurements. In addition, a *Hirsutella*-like synanamorph recovered from ARSEF 14590 yielded uniseptate conidia that exceeded the spore length maximum for all previously measured CL strains. Host associations for a majority of isolates were taxonomically unresolved below family level, so it remains unclear whether there are any biologically significant patterns across CL and *Conoideocrella*. Consistent with previous literature (Saito et al. 2012), we found that nonsessile crawlers are more vulnerable to infection, which may present challenges for identifying insects based on diagnostically relevant morphological characteristics often described from adults (Urbina and Ahmed 2022). Even under ideal conditions for identifying the host (i.e., when adults are infected), CL quickly envelops and significantly degrades hosts, making their morphological identification below family level impractical (Hywel-Jones 1993).

CL monophyly, and its relationship with CT, was well supported in both the larger Clavicipitaceae data set and the *Conoideocrella*-focused data set, but none of our analyses support the monophyly of *Conoideocrella*, with various and incongruent placement of CK and DT. The exclusion of DT from the recent taxonomic description of CK resulted in a well-supported, but incomplete perspective of the genetic relationships among the three species of *Conoideocrella*. Both the historical and current morphological data generated for this study provide further insights, some of which further support our phylogenetic conclusions: CK has noticeably different ascospore lengths compared with CL, CT, and DT according to the literature (TABLE 4). On the other hand, CK and CL both produced *Hirsutella*-like anamorphs with occasionally (CL) to exclusively (CK)

septate conidia singly or in pairs on unbranched short conidiophores. Although this synanamorph was only produced by CL under special circumstances, it produced mostly aseptate conidia similar in size to those reported for the *Paecilomyces*-like synanamorph seen in all examined CL strains. DT also produces a similar *Hirsutella*-like or sphacelia-like asexual state with aseptate to occasionally uniseptate conidia on "needle-shaped" conidiophores (Atkinson 1891). Despite the presence of a *Hirsutella*-like anamorph in our North Carolina CL strains, the *Paecilomyces*-like synanamorph with aseptate conidia on verticillate conidiophores was the dominant anamorph and observed in all examined strains. Whether CL, CT, and DT, or all *Conoideocrella* spp. including CK and DT should be synonymized as *Dussiella* spp. remains unclear without additional sequence data and conidiophore and conidial observations and measurements for CT. These are currently lacking, as are morphological and molecular data sets for a CL-like fungus that was commonly reported on various insect hosts across the southeastern U.S. in the first half of the last century (see TABLE 1). To tackle these issues, future researchers investigating fungal epizootics on Hemiptera should retain sufficient materials for morphological investigations, DNA sequencing including *EF1*-α and other protein-coding genes including *RPB1* and *RPB2*, and depositing voucher specimens in herbaria for future independent examination. The paucity of sequence data for *Dussiella* will require targeted sequencing of strains from culture collections and herbaria as well as robust field sampling. Furthermore, sequencing of *COX1* (cytochrome c oxidase I) from mycosed scale insect/whitefly cadavers, whether by *Conoideocrella, Dussiella*, or *Aschersonia*, may permit sub-family-level identification in the absence of diagnostic morphological features.

The possible occurrence of a *Paecilomyces*-like synanamorph in CK, CT, and DT should also be thoroughly investigated, as should the presence of a *Hirsutella*-like synanamorph in CT. The co-occurence of both types of conidiophores in ARSEF 14590 indicates that both can be produced contemporaneously under certain conditions and might explain the much wider range of conidial measurements for CK, regardless of whether it is a valid *Conoideocrella* sp. or a closely allied novel genus that is yet to be designated.

Although both synanamorphs of CL grew sufficiently at ~20 C, as did the *Hirsutella*-like anamorph of CK, growth rates provided by Mongkolsamrit et al. (2016) for CK show significantly reduced growth for the *Hirsutella*-like synanamorph compared with the *Paecilomyces*-like synanamorph for CL reported by Saito et al. (2012) and in this study. More work is needed to determine optimal temperature ranges for growth, sporulation, and spore germination for both asexual forms, especially CL's *Hirsutella*-like synanamorph, which was only recently uncovered. Despite the overlap in growth conditions, each may be adapted for different seasons, host developmental stages, or both given the absence of a sexual stage in the U.S. and Japan. How these temperatures overlap with temperature optima for EHS is also significant. Following the introduction of EHS into the U.S., populations adapted to expand into colder regions (Preisser et al. 2008). Whereas adult female EHS can be found year round, crawlers are present from spring through autumn. Considering these factors, CL application as a biopesticide may be most effective in early spring, with the aim to establish an epizootic that controls crawlers throughout their emergence.

Although much work has been done on the taxonomy of *Torrubiella* and closely allied fungi over the last decade and a half (Sung et al. 2007; Johnson et al. 2009), some taxonomic uncertainties in and around *Conoideocrella* remain. Most importantly, Petch (1923) noted that he had not examined the type specimen of CL described by Zimmermann (1901) from Java, so how the morphology and phylogenetic placement of this specimen overlaps with our current understanding of CL requires further scrutiny. This is especially relevant because Zimmermann noted that part-ascospores were not observed in Java type material, whereas Petch noted cylindrical part-spores from several locations (Petch 1923). The placement of *Torrubiella brunnea* also suffers from taxonomic uncertainty (Petch 1923; Hywel-Jones 1993).

Despite the urgent need for a major taxonomic revision of *Conoideocrella, Dussiella*, and closely allied genera, it is clear that CL is well defined as a species and is currently the only *Conoideocrella* species for which pathogenicity has been formally tested. Saito et al. (2012) confirmed pathogenicity of CL on *Camellia* spiny whitefly nymphs using three Japanese strains. The results of their bioassays not only revealed significant differences in infection rates across strains and inoculum concentrations, but also that CL outperformed commercially available mycoinsecticides at concentrations below recommended field application rates for those products (Saito et al. 2012). Although pathogenicity was confirmed using our North Carolina CL strains against EHS, reduced infection rates compared with Japanese CL strains on whitefly might be explained by multiple factors: (i) our bioassays were conducted over a 2-week period compared with a 3-week period for whitefly bioassays, which showed significant jumps in infection rates between weeks 2 and 3; and (ii) our

bioassay used a single (medium) concentration treatment [against EHS] that failed to cause higher infection rates against whiteflies using Japanese CL strains for two of three strains compared with the negative control after 2 weeks (Saito et al. 2012). Given the close phylogenetic relationship between U.S. and Japanese strains, it is plausible that whiteflies may serve as the preferred host over armored scale insects despite the confirmed susceptibility of various members of Coccidae, Diaspididae, and Aleyrodidae. Given the numerous records from the U.S. Southeast from whiteflies between 1913 and 1939, surveys to recover and characterize CL from whiteflies including assessing pathogenicity are urgently needed.

The lack of reports of CL, especially from whiteflies, from the early 1940s through the 2010s is perplexing. One possible explanation is that CL may have been mistaken for another entomopathogenic fungal genus that infects whiteflies, *Aschersonia*, which has been reported widely in the southeastern U.S since the early 20th century. Both produce orange-colored stroma atop infected insects on the underside of leaves (Fasulo and Weems 1999; Martini et al. 2022). Otherwise, the absence of CL observations during this prolonged time period may reflect (i) a gradual, albeit unchecked decades-long host expansion of CL from whiteflies in the southeastern U.S. to armored scale insects possibly due to declining citrus whitefly populations; (ii) a precipitous drop in EHS's primary host (eastern hemlock) due to mortality from hemlock woolly adelgid across most of the introduced range of EHS; (iii) a relatively recent jump by EHS to Christmas trees (firs) that may support higher densities of EHS or unique microsite conditions compared with eastern hemlock, thus allowing for the emergence of an epizootic; (iv) an increase in classical biocontrols, including *Encarsia citrina*, a parasitoid wasp of adult EHS, and *Cybocephalus nipponicus*, a beetle predator of EHS, which were found among CL-infected EHS in North Carolina and may spread conidia; and/or (v) changes in management, particularly the use of insecticides that impacted fungal growth.

Insect growth regulators such as buprofezin have provided the most consistent and long-lasting control against EHS in Christmas tree farms (Sidebottom 2016). Coincidentally, comparisons among 17 commercial insecticides on CL growth showed buprofezin and 11 other insecticides significantly reduced fungal growth (Saito et al. 2012), which might account for the lack of previous observations in these treated stands. Interestingly, most of the sites where CL was detected were on farms where management had been abandoned, including the use of insecticides. On the other hand, imidacloprid, which is commonly used to treat HWA and EHS, had no effect on growth of CL (Saito et al. 2012), assuming adequate healthy populations of EHS exist in an area to sustain fungal populations. The preferential use of imidacloprid in hemlock forests and buprofezin in Christmas tree farms may allow CL to survive in areas adjacent to Christmas tree farms.

Our study provides important historical context for understanding this modern CL epizootic among EHS in U.S. Christmas tree farms. CL has been observed infecting insects across the eastern U.S. since the early 1900s. The observed host range of CL includes multiple economically important pest insects but lacks insects that would be considered beneficial. The primary spore CL produces in artificial culture is infective to the primary motile stage of EHS, which is key for the spread of this pest insect in Christmas tree farms. Motile stages are also more likely to encounter an applied biopesticide. Multiple factors, including Christmas tree management practices, may contribute to recent and conspicuous outbreaks among U.S. EHS populations. Considering the developmental stage specificity of CL, its integration as a biocontrol intervention against EHS would be most effective just before and throughout crawler emergence. Development of CL for applied use by the Christmas tree industry may help alleviate the burden of EHS on tree export; however, the potential of this product may extend beyond Christmas tree orchards controlling other pest insects.

ACKNOWLEDGMENTS

We acknowledge that this work was completed on the traditional land of the Osage, Shawnee, and Massawomeck peoples. Samples were additionally collected on the land of Cherokee, Yuchi, and Moneton peoples. We especially thank Ryan Percifield, Director of the West Virginia University Genomics Core Facility, who assisted with library preparation and sequencing of *C. luteorostrata* strain ARSEF 14590.

DISCLOSURE STATEMENT

JES was a paid consultant for Zymergen, Sincarne, and Michroma.

FUNDING

This project was funded by the Christmas Tree Promotion Board grants 20-10-WVU and 21-07-WVU. B.L. was supported by the U.S. Department of Agriculture (USDA-ARS Project 8062-22410-007-000D). H.B. was supported by West Virginia University (WVU) Research Apprentice Program, and the Honors Biology Capstone Program, under Dr. Susan Raylman in the WVU Department of Biology. A.M.M. was supported by a WVU Outstanding Merit Fellowship. J.E.S. is

a Canadian Institute for Advanced Research (CIFAR) fellow in the program "Fungal Kingdom: Threats and Opportunities" and was supported by the National Science Foundation (NSF) (EF-2125066) and the U.S. Department of Agriculture (USDA) (National Institute of Food and Agriculture Hatch project CA-R-PPA-211-5062-H). Analyses were performed on the University of California Riverside High Performance Computing Cluster supported by the NSF (DBI-1429826 and DBI-2215705) and the National Institutes of Health (NIH) (S10-OD016290).

ORCID

Brian Lovett http://orcid.org/0000-0002-5721-7695
Angie M. Macias http://orcid.org/0000-0002-2975-686X
Jason E. Stajich http://orcid.org/0000-0002-7591-0020
Matt T. Kasson http://orcid.org/0000-0001-5602-7278

LITERATURE CITED

Artjariyasripong S, Mitchell JI, HyweI-Jones NL, Jones EBG. 2001. Relationship of the genus cordyceps and related genera, based on parsimony and spectral analysis of partial 18S and 28S ribosomal gene sequences. Mycoscience. 42 (6):503–517.

Atkinson GF. 1891. On the structure and dimorphism of *Hypocrea tuberiformis*. Bot Gazette. 16(10):282–285.

Chechi A, Stahlecker J, Dowling M, Schnabel G. 2019. Diversity in species composition and fungicide resistance profiles in *Colletotrichum* isolates from apples. Pestic. Biochem. Physiol. 158:18–24. doi:10.1016/j.pestbp.2019.04.002.

Dale AG, Birdsell T, Sidebottom J. 2020. Evaluating the invasive potential of an exotic scale insect associated with annual Christmas tree harvest and distribution in the southeastern U.S. Trees Forest People. 2:100013. doi:10.1016/j.tfp.2020.100013.

de Mendiburu F. 2021. *Agricolae*: statistical procedures for agricultural research. R package version. 1.3–5. https://CRAN.R-project.org/package=agricolae.

Fasulo TR, Weems HV 1999. Featured creatures: citrus whitefly. University of Florida IFAS Extension Publication Publication Number: EENY-84. https://entnemdept.ufl.edu/creatures/citrus/citrus_whitefly.htm

Fox J, Weisberg S. 2019. An R companion to applied regression. 3rd ed. Thousand Oaks (CA, USA): Sage.

Gao T, Wang Z, Huang Y, Keyhani NO, Huang Z. 2017. Lack of resistance development in *Bemisia tabaci* to *Isaria fumosorosea* after multiple generations of selection. Sci Rep. 7 (1):42727. doi:10.1038/srep42727.

Garnier S, Ross N, Rudis R, Camargo AP, Sciaini M, Scherer C. 2021. *Rvision* - colorblind-friendly color maps for R. R package version 0.6.2. https://github.com/swarm-lab/Rvision.

Gavrilov-Zimin IA, Borisov BA. 2020. *Aleuroclava aucubae* (Homoptera: Aleyrodinea), a new adventive species for Russian Black Sea Coast, and its concomitant entomoparasitic fungus *Conoideocrella luteorostrata* (Ascomycota: hypocreales: clavicipitaceae). Zoosystematica Rossica. 29 (1):3–10. doi:10.31610/zsr/2020.29.1.3.

Hywel-Jones NL. 1993. *Torrubiella luteorostrata*: a pathogen of scale insects and its association with *Paecilomyces cinnamomeus* with a note on *Torrubiella tenuis*. Mycol Res. 97 (9):1126–1130. doi:10.1016/S0953-7562(09)80514-5.

Ivic D, Voncina D, Sever Z, Simon S, Pejic I. 2013. Identification of *Colletotrichum* species causing bitter rot of apple and pear in Croatia. J. Phytopathol. 161 (4):284–286. doi:10.1111/jph.12039.

Johnson D, Sung GH, Hywel-Jones NL, Luangsa-Ard JJ, Bischoff JF, Kepler RM, Spatafora JW. 2009. Systematics and evolution of the genus *Torrubiella* (Hypocreales, Ascomycota). Mycol. Res. 113(3):279–289. doi:10.1016/j.mycres.2008.09.008.

Kasson MT, Pollok JR, Benhase EB, Jelesko JG. 2014. First report of seedling blight of eastern poison ivy (*Toxicodendron radicans*) by *Colletotrichum fioriniae* in Virginia. Plant Dis. 98(7):995–995. doi:10.1094/PDIS-09-13-0946-PDN.

Katoh K, Standley DM. 2013. MAFFT multiple sequence alignment software version 7: improvements in performance and usability. Mol Biol Evol. 30(4):772–780.

Kepler RM, Sung GH, Harada Y, Tanaka K, Tanaka E, Hosoya T, Bischoff JF, Spatafora JW. 2012. Host jumping onto close relatives and across kingdoms by Tyrannicordyceps (clavicipitaceae) gen. nov. And Ustilaginoidea_ (clavicipitaceae). Am J Bot. 99(3):552–561.

Koroch A, Juliani H, Bischoff J, Lewis E, Bills G, Simon J, White JR. 2004. Examination of plant biotrophy in the scale insect parasitizing fungus *Dussiella tuberiformis*. Symbiosis. 37:267–280.

Landan G, Graur D. 2008. Local reliability measures from sets of co-optimal multiple sequence alignments. In Biocomputing 2008. (p. 15–24).

Li DW, Cowles RS, Vossbrinck CR. 2008. *Metarhiziopsis microspora* gen. et sp. nov. associated with the elongate hemlock scale. Mycologia. 100(3):460–466. doi:10.3852/07-078R1.

Ling JF, Peng AT, Jiang ZD, Xi PG, Song XB, Cheng BP, Cui YP, Chen X. 2021. First report of anthracnose fruit rot caused by *Colletotrichum fioriniae* on Litchi in China. Plant Dis. 105(4):1225. doi:10.1094/PDIS-07-20-1539-PDN.

Luangsa-ard JJ, Tasanathai K, Mongkolsamrit S, Hywel-Jones NL. 2007. Atlas of invertebrate-pathogenic fungi of Thailand. Biotec. NSTDA Thailand.

Macias AM, Geiser DM, Stajich JE, Łukasik P, Veloso C, Bublitz DC, Berger MC, Boyce GR, Hodge K, Kasson MT. 2020. Evolutionary relationships among *Massospora* spp. (Entomophthorales), obligate pathogens of cicadas. Mycologia. 112(6):1060–1074. doi:10.1080/00275514.2020.1742033.

Manni M, Berkeley MR, Seppey M, Simão FA, Zdobnov EM. 2021. BUSCO update: novel and streamlined workflows along with broader and deeper phylogenetic coverage for scoring of eukaryotic, prokaryotic, and viral genomes. Mol Biol Evol. 38(10):4647–4654. doi:10.1093/molbev/msab199.

Marcelino JAP, Gouli S, Parker BL, Skinner M, Giordano R. 2009. Entomopathogenic activity of a variety of the fungus, *Colletotrichum acutatum*, recovered from the elongate hemlock scale, *Fiorinia externa*. J Insect Sci. 9(1):13. doi:10.1673/031.009.1301.

Martini X, Diepenbrock LM, Ray KL, Burrow JD. 2022. Citrus pest quick guide: citrus whitefly (*Dialeurodes citri*). University of Florida IFAS Extension Publication Number: ENY-2037. https://edis.ifas.ufl.edu/publication/in1322.

Martin PL, Peter KA. 2021. Quantification of *Colletotrichum fioriniae* in orchards and deciduous forests indicates it is primarily a leaf endophyte. Phytopathology. 111 (2):333–344. doi:10.1094/PHYTO-05-20-0157-R.

McClure MS. 1977a. Resurgence of the scale, *Fiorinia externa* (Homoptera: Diaspididae), on hemlock following insecticide application. Environ Entomol. 6(3):480–484. doi:10.1093/ee/6.3.480.

McClure MS. 1977b. Parasitism of the scale insect, *Fiorinia externa* (Homoptera: Diaspididae), by *Aspidiotiphagus citrinus* (Hymenoptera: Eulophidae) in a hemlock forest: density dependence. Environ Entomol. 6(4):551–555. doi:10.1093/ee/6.4.551.

McClure MS, Fergione MB. 1977. *Fiorinia externa* and *Tsugaspidiotus tsugae* (Homoptera: diaspididae): distribution, abundance, and new hosts of two destructive scale insects of eastern hemlock in Connecticut. Environ Entomol. 6(6):807–811. doi:10.1093/ee/6.6.807.

Miller DR, Davidson JA. 2005. Armored scale insect pests of trees and shrubs (Hemiptera: diaspididae). Ithaca: NY (USA): Cornell University Press; p. 200–202.

Mongkolsamrit S, Thanakitpipattana D, Khonsanit A, Promharn R, Luangsa-ard JJ. 2016. sp. nov., an entomopathogenic fungus from Thailand. Mycoscience. 57 (4):264–270. doi:10.1016/j.myc.2016.03.003.

Morrill AW, Back EA. 1911. White flies injurious to citrus in Florida (No. 92). US Department of Agriculture, Bureau of Entomology.

Neuwirth E 2022. *RColorBrewer*: colorBrewer palettes. R package version 1.1-3. https://CRAN.R-project.org/package=RColorBrewer.

Petch T. 1923. Studies in entomogenous fungi: III. Torrubiella. Trans Br Mycol Soc. 9(1):108–128. doi:10.1016/S0007-1536(23)80018-3.

Preisser EL, Elkinton JS, Abell K. 2008. Evolution of increased cold tolerance during range expansion of the elongate hemlock scale *Fiorinia externa* Ferris (Hemiptera: diaspididae). Ecol Entomol. 33(6):709–715. doi:10.1111/j.1365-2311.2008.01021.x.

Rambaut A, Drummond AJ, Xie D, Baele G, Suchard MA. 2018. Posterior summarisation in Bayesian phylogenetics using Tracer 1.7. Syst Biol. 67(5):901–904. doi:10.1093/sysbio/syy032.

R Core Team. 2022. R: a language and environment for statistical computing. Vienna (Austria): R Foundation for Statistical Computing. https://www.R-project.org/

Rehner SA, Samuels GJ. 1994. Taxonomy and phylogeny of *Gliocladium* analyzed from nuclear large subunit ribosomal DNA sequences. Mycol Res. 98(6):625–634. doi:10.1016/S0953-7562(09)80409-7.

Rivalier E, Seydel S. 1932. Nouveau procedé de culture sur lames gélosées applique a l'étude microscopique des champignons des teignes. Annales de Parasitologie Humaine et Comparee. 10(5):444–452. doi:10.1051/parasite/1932105444.

Ronquist F, Teslenko M, van der Mark P, Ayres DL, Darling A, Höhna S, Larget B, Liu L, Suchard MA, Huelsenbeck JP. 2012. MrBayes 3.2: efficient Bayesian phylogenetic inference and model choice across a large model space. Systematic Biology. 61(3):539–542. doi:10.1093/sysbio/sys029.

Royle DD, Lathrop RG. 2002. Discriminating *Tsuga canadensis* hemlock forest defoliation using remotely sensed change detection. Journal of Nematology. 34(3):213–221.

Saito T, Takatsuka J, Shimazu M. 2012. Characterization of *Paecilomyces cinnamomeus* from the camellia whitefly, *Aleurocanthus camelliae* (Hemiptera: Aleyrodidae), infesting tea in Japan. J Invertebr Pathol. 110(1):14–23. doi:10.1016/j.jip.2012.01.011.

Samson RA. 1974. *Paecilomyces* and some allied hyphomycetes. Stud Mycol. 6:1–119.

Sasscer ER. 1912. The genus *Fiorinia* in the United States. USDA Technical Series no. 16 part 5. In: USDA, Bureau of Entomology, editor. Papers on Coccidae or scale insects. Washington DC (USA): Government Printing Office. p. 75–82.

Schoch CL, Ciufo S, Domrachev M, Hotton CL, Kannan S, Khovanskaya R, Leipe D, Mcveigh R, O'Neill K, Robbertse B, et al. 2020. NCBI taxonomy: a comprehensive update on curation, resources and tools. Database. 2020:1–21. doi:10.1093/database/baaa062.

Sela I, Ashkenazy H, Katoh K, Pupko T. 2015. GUIDANCE2: accurate detection of unreliable alignment regions accounting for the uncertainty of multiple parameters. Nucl Acid Res. 43(W1):W7–W14. doi:10.1093/nar/gkv318.

Sidebottom J. 2016 (revised 2019). Elongate hemlock scale. NC State University Extension Christmas Tree Notes. North Carolina State University Cooperative Extension. https://content.ces.ncsu.edu/elongate-hemlock-scale.

Stajich JE, Palmer J. 2019. Automatic assembly for the fungi (AAFTF): genome assembly pipeline. Version 0.4.1. Zenodo.

Stamatakis A. 2014. RAxML version 8: a tool for phylogenetic analysis and post-analysis of large phylogenies. Bioinformatics. 30(9):1312–1313. doi:10.1093/bioinformatics/btu033.

Sung GH, Sung JM, Hywel-Jones NL, Spatafora JW. 2007. A multi-gene phylogeny of Clavicipitaceae (Ascomycota, fungi): identification of localized incongruence using a combinational bootstrap approach. Mol Phylogenet Evol. 44(3):1204–1223.

Tamura K, Stecher G, Kumar S. 2021. MEGA11: molecular evolutionary genetics analysis version 11. Mol Biol Evol. 38 (7):3022–3027. doi:10.1093/molbev/msab120.

Therneau T. 2022. A package for survival analysis in R. R package version 3.4-0. https://CRAN.R-project.org/package=survival.

Urbina H, Ahmed MZ. 2022. Characterization of the entomopathogenic fungal species *Conoideocrella luteorostrata* on the scale insect pest *Fiorinia externa* infesting the Christmas tree *Abies fraseri* in the USA. Florida Entomol. 5(1):10–21.

Vilgalys R, Hester M. 1990. Rapid genetic identification and mapping of enzymatically amplified ribosomal DNA from several *Cryptococcus* species. J Bacteriol. 172(8):4238–4246. doi:10.1128/jb.172.8.4238-4246.1990.

Villamizar LF, Barrera G, Hurst M, Glare TR. 2021. Characterization of a new strain of *Metarhizium novozealandicum* with potential to be developed as a biopesticide. Mycology. 12(4):261–278. doi:10.1080/21501203.2021.1935359.

White JF, Jr, Belanger F, Meyer W, Sullivan RF, Bischoff J, Lewis E. 2002. Clavicipitalean fungal epibionts and endophytes–development of symbiotic interactions with plants. Symbiosis. 33(3):201–213.

White TJ, Bruns T, Lee S, Taylor J. 1990. Amplification and direct sequencing of fungal ribosomal RNA genes for phylogenetics. In: Innis MA, Gelfand DH, Sninsky JJ, White TJ, editors. PCR protocols: a guide to methods and applications. New York (NY, USA): Academic Press, Inc. p. 315–322.

Wickham H, Averick M, Bryan J, Chang W, McGowan LD, François R, Grolemund G, Hayes A, Henry L, Hester J, et al. 2019. Welcome to the tidyverse. J Open Source Softw. 4 (43):1686. doi:10.21105/joss.01686.

Wickham H, Seidel D 2022. *scales*: scale functions for visualization. R package version 1.2.1. https://CRAN.R-project.org/package=scales.

Zimmermann A. 1901. Zentralblatt für Bakteriologie, Parasitenkunde und Infektionskrankheiten 1. Abt. 7:872.